PL-TR-93-2128

COHERENT HF RADAR SYSTEM FOR THE STUDY OF NATURAL AND HEATER INDUCED IONOSPHERIC IRREGULARITIES

Bodo W. Reinisch
James L. Scali
D. Mark Haines

University of Massachusetts Lowell
Center for Atmospheric Research
450 Aiken Street
Lowell, MA 01854

June 1993

Final Report

August 1991 - May 1993

PHILLIPS LABORATORY
Directorate of Geophysics
AIR FORCE MATERIEL COMMAND
HANSCOM AIR FORCE BASE, MA 01731-3010

"This technical report has been reviewed and is approved for publication."

B. S. Dandekar
Contract Manager
Branch

Maj Edward Bergborn, Chief
Ionospheric Application

WILLIAM K. VICKERY, Director
Ionospheric Effects Division

This report has been reviewed by the ESC Public Affairs Office (PA) and is releasable to the National Technical Information Service (NTIS).

Qualified requestors may obtain additional copies from the Defense Technical Information Center (DTIC). All others should apply to the National Technical Information Service (NTIS).

If your address has changed, or if you wish to be removed from the mailing list, or if the addressee is no longer employed by your organization, please notify PL/TSI, 29 Randolph Road, Hanscom AFB, MA 01731-3010. This will assist us in maintaining a current mailing list.

Do not return copies of this report unless contractual obligations or notices on a specific document requires that it be returned.

REPORT DOCUMENTATION PAGE

Form Approved
OMB No. 0704-0188

1. AGENCY USE ONLY (Leave blank)	2. REPORT DATE	3. REPORT TYPE AND DATES COVERED
	June 1993	Final Report, Aug 1991-May 1993

4. TITLE AND SUBTITLE
Coherent HF Radar System for the Study of Natural and Heater Induced Ionospheric Irregularities

5. FUNDING NUMBERS
PE 61102F
PR 4029 TA01 WUAD
Contract No.
F19628-91-K-0036

6. AUTHOR(S)
Bodo W. Reinisch
James L. Scali
D. Mark Haines

7. PERFORMING ORGANIZATION NAME(S) AND ADDRESS(ES)
University of Massachusetts Lowell
Center for Atmospheric Research
450 Aiken Street
Lowell, MA 01854

8. PERFORMING ORGANIZATION REPORT NUMBER

9. SPONSORING/MONITORING AGENCY NAME(S) AND ADDRESS(ES)
Phillips Laboratory
29 Randolph Road
Hanscom AFB, MA 01731-3010

Contract Manager: B. S. Dandekar/GPIS

10. SPONSORING/MONITORING AGENCY REPORT NUMBER
PL-TR-93-2128

11. SUPPLEMENTARY NOTES

12a. DISTRIBUTION/AVAILABILITY STATEMENT
Approved for public release;
distribution unlimited

12b. DISTRIBUTION CODE

13. ABSTRACT *(Maximum 200 words)*

The highly irregular polar ionosphere requires sophisticated sensing techniques to identify and monitor the ionospheric characteristics. This report describes the deployment of a new ionospheric sounder, the Digisonde Portable Sounder (DPS), at Svalbard (78.2°N) and discusses the first results obtained with this instrument. The most important new feature in the DPS, not available in the old Digisondes, is the capability of high precision incidence angle measurements and spectral characterization at up to 128 ranges.

While Svalbard rotated from the polar cap (at magnetic midnight) through the reversal boundaries and the auroral oval to the cusp region, the DPS was able to monitor the different features of a highly stressed ionosphere. It is demonstrated that the DPS can characterize the behavior of the background ionosphere while simultaneously measuring the motion of irregular plasma structures. This capability can be applied to identify and track irregularities generated by high power HF transmitters as planned for HAARP (HF Active Auroral Research Program) experiments in Alaska. This report shows how the DPS identifies different plasma structures in a naturally stressed ionosphere within the field of view of the instrument which extends over several hundred kilometers in the ionosphere.

14. SUBJECT TERMS	15. NUMBER OF PAGES
Electron Density, Plasma Structure, Plasma Convection, Digisonde Portable Sounder, HF Active Auroral Research Program (HAARP)	50
	16. PRICE CODE

17. SECURITY CLASSIFICATION OF REPORT	18. SECURITY CLASSIFICATION OF THIS PAGE	19. SECURITY CLASSIFICATION OF ABSTRACT	20. LIMITATION OF ABSTRACT
Unclassified	Unclassified	Unclassified	SAR

Table of Contents

List of Illustrations

List of Illustrations

1.0 INTRODUCTION

Highly turbulent, irregular, or "stressed" ionospheres are observed in polar regions, especially in the shear flow regimes of the cusp, at the trailing edges of polar cap patches, in the shears associated with auroral F-layer arcs, in the post sunset equatorial plumes, and manmade during high powered heating experiments. Modern techniques are required to characterize the parameters of the stressed plasma in order to develop an understanding of the plasma process involved. These measurements are especially difficult in the above listed scenarios, since the structure of the irregular plasma has to be measured while the background ionosphere itself is irregular and often moving or drifting at high velocities. This report demonstrates the capability of the Digisonde Portable Sounder (DPS) to measure the characteristics of the stressed ionospheric environment. The overall contract comprised the building and installation of a Digisonde Portable Sounder and the subsequent demonstration that the DPS can monitor the naturally stressed ionosphere at Svalbard.

Such observations are directly applicable to the ionospheric modification experiments to be conducted under the Joint Services HF Active Auroral Research Program (HAARP) in Alaska. The DPS characterizes the bulk parameters of the ionosphere including changes of the electron density, plasma structure and the plasma convection. In the absence of the HAARP facility at the present time, the high latitude ionosphere at Svalbard is used as a natural plasma laboratory to demonstrate the DPS. The DPS monitors the development of plasma irregularities in response to various stressing factors such as electric fields, plasma flow shears and particle precipitation.

This development and research was performed in two phases: phase one for the building and installing the DPS covering two quarters of the twenty-one months contract and phase two for the monitoring of the naturally stressed ionospherc at Svalbard covering the balance of the contract. This report provides an overview of the tasks completed as well as a summary of the scientific evaluation of the data collected.

2.0 DIGISONDE PORTABLE SOUNDER

The Digisonde Portable Sounder (Reinisch et al., 1991), referred to as the DPS, is a self contained, low cost digital ionosonde. The DPS simultaneously measures frequency, height/range (time delay), amplitude, phase, Doppler shift or spread (frequency dispersion), wave polarization (left or right hand) and angle of arrival. The DPS can display as many as five of these parameters at any one time. One advantage of the DPS compared to the Digisonde 256 is the reduced peak pulse power of 300W, another is the ability to determine complete 128 line spectra for all 128 range gates. This latter feature is of importance for the monitoring of "heated' regions in the HAARP environment (see discussion on page 20). An array of four polarized receiving loop antennas with preamplifiers and polarization switches are connected to the DPS via 50Ω cables.

The real-time control of the DPS hardware is implemented by an embedded 80386 based microcomputer connected to a digitizer and signal processor as well as to the custom hardware which implements the ionospheric sounder waveform generator and transceiver. The real-time control functions include sequencing of frequencies, selection of transmitter waveform, selection of receive antenna configuration, selection of receiver gain, control of data acquisition, control of the parallel digital signal processor (DSP) and transferring of data. These functions are implemented by software written in C with calls to high speed assembly language subroutines which transfer data to/from the digitizer, DSP card and the DPS chassis hardware.

2.1 Initial Design and Deployment

At the start of the contract and through the deployment, the DPS was developed as a dual chassis unit containing the DPS circuitry (with the exception of the frequency synthesizer) in one 19" rack mounted chassis and the transmitter power amplifier placed in a second 19" rack mounted chassis. The frequency synthesis was accomplished through a third commercial chassis, controlled by the DPS chassis. The frequency synthesizer used was manufactured by Programmed Test Sources, model PTS 160. The three chassis were integrated into a single fiberglass enclosure for ease of transport. Figure 1 shows the configuration of the chassis in the enclosure. Peripheral equipment for the DPS include a color VGA monitor, Hewlett Packard color printer, Okidata dot matrix printer and keyboard. The system receives

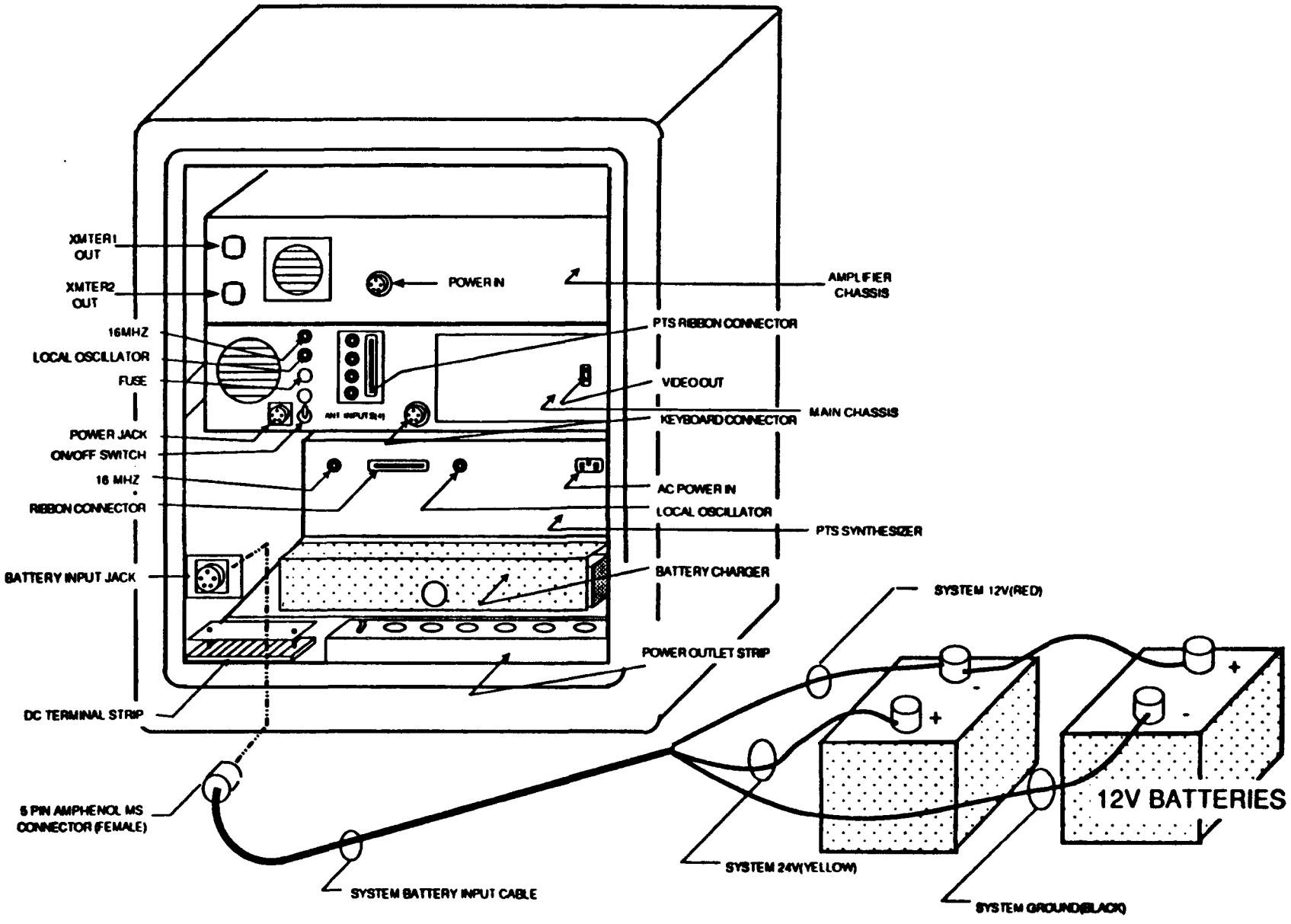

Figure 1. Digisonde Portable Sounder (S/N 01) System Configuration.

primary power from two 12V lead acid batteries that are trickle charged through two Lambda power supplies. The system was configured for 110VAC, however, the system was deployed with a 220/110VAC step down transformer for compatibility in the Svalbard power environment.

Figure 2 presents the chassis layout of the two chassis and Figure 3 presents a system block diagram of the DPS architecture. In Figure 3 the blocks with a bold border and the antenna switch are circuit card assemblies designed by the ULCAR staff. The Digital Signal Processor is manufactured by Bridgenorth, Model BN2500, and the Digitizer is manufactured by RC Electronics, Model ICS-16R.

The DPS (serial number 01) completed final assembly and test in November 1991. The peripheral equipment were shipped to Svalbard via commercial air freight. The DPS enclosure was hand carried to Svalbard by ULCAR engineer Mr. D. Mark Haines in December. On arrival in Svalbard, Mr. Haines and Messers. Terry Bullett and Les Pedin, Phillips Laboratory, installed and operated the DPS system. On departure of Messers Haines, Bullett and Pedin the DPS was fully operational. Specifics of the system installation are detailed in Quarterly Status Report Number 2, dated April 8, 1993. The DPS System Technical Manual gives a detailed description of the system and its operation.

2.2 System Upgrade

The DPS operated successfully for the following year but showed some deficiencies requiring correction. The system was unable to distinguish between vertical and off-vertical echoes in the ionogram which frequently made it impossible for ARTIST to extract the correct foF2 frequencies. New software available at ULCAR was not compatible with the commercial digitizer in the Ny Alesund DPS. ULCAR had in the meantime designed a new Digitizer card, that is adaptable to a one or four receiver configuration, and the new software required the new Digitizer. Also during the year's operation, the design of the DPS had advanced in that the commercial Frequency Synthesizer had been replaced by an ULCAR designed printed circuit card. With this latest design enhancement, the PTS synthesizer was no longer required and could be completely replaced with the ULCAR Synthesizer card.

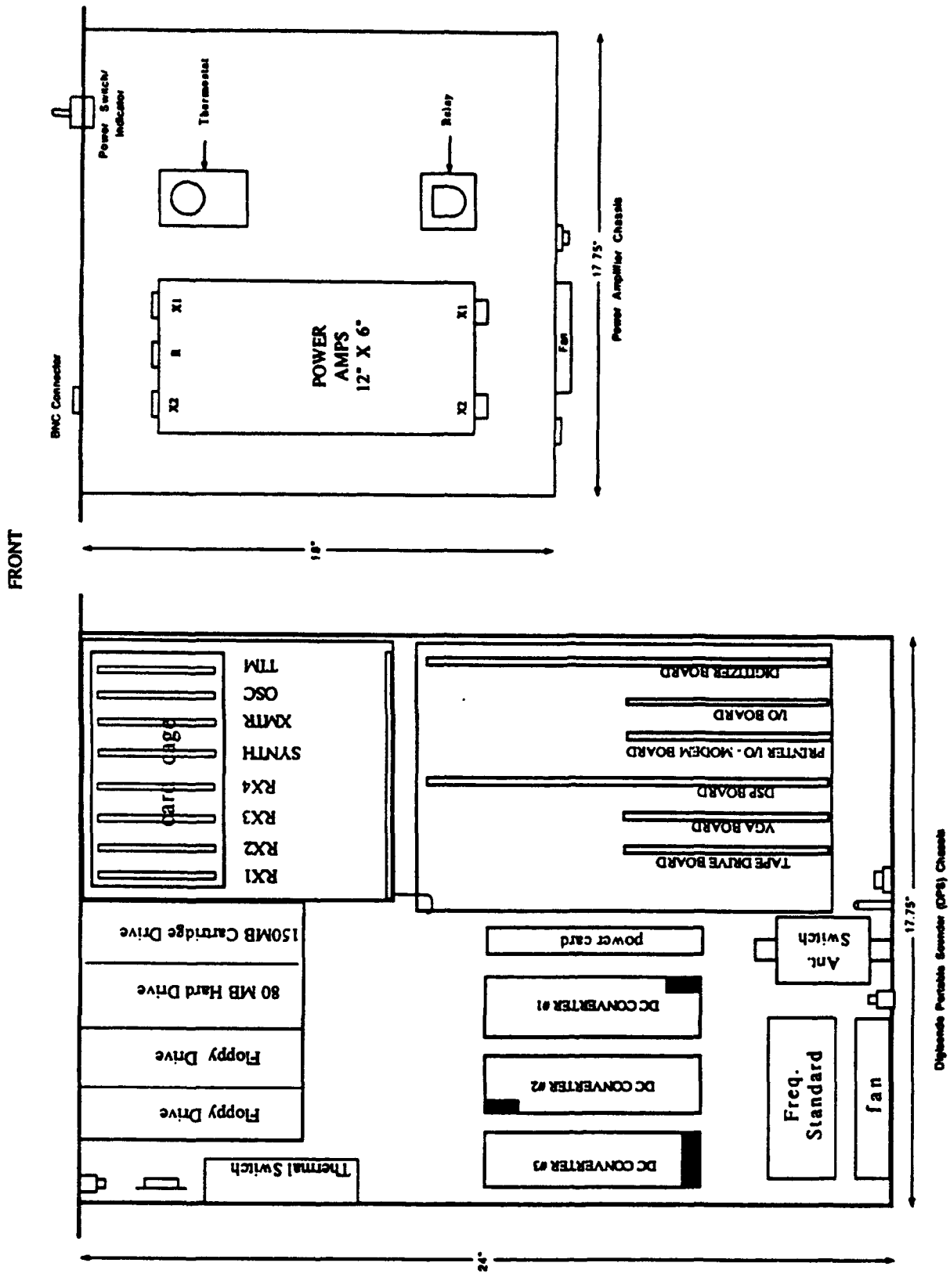

Figure 2. Digisonde Portable Sounder (S/N 01) System Components.

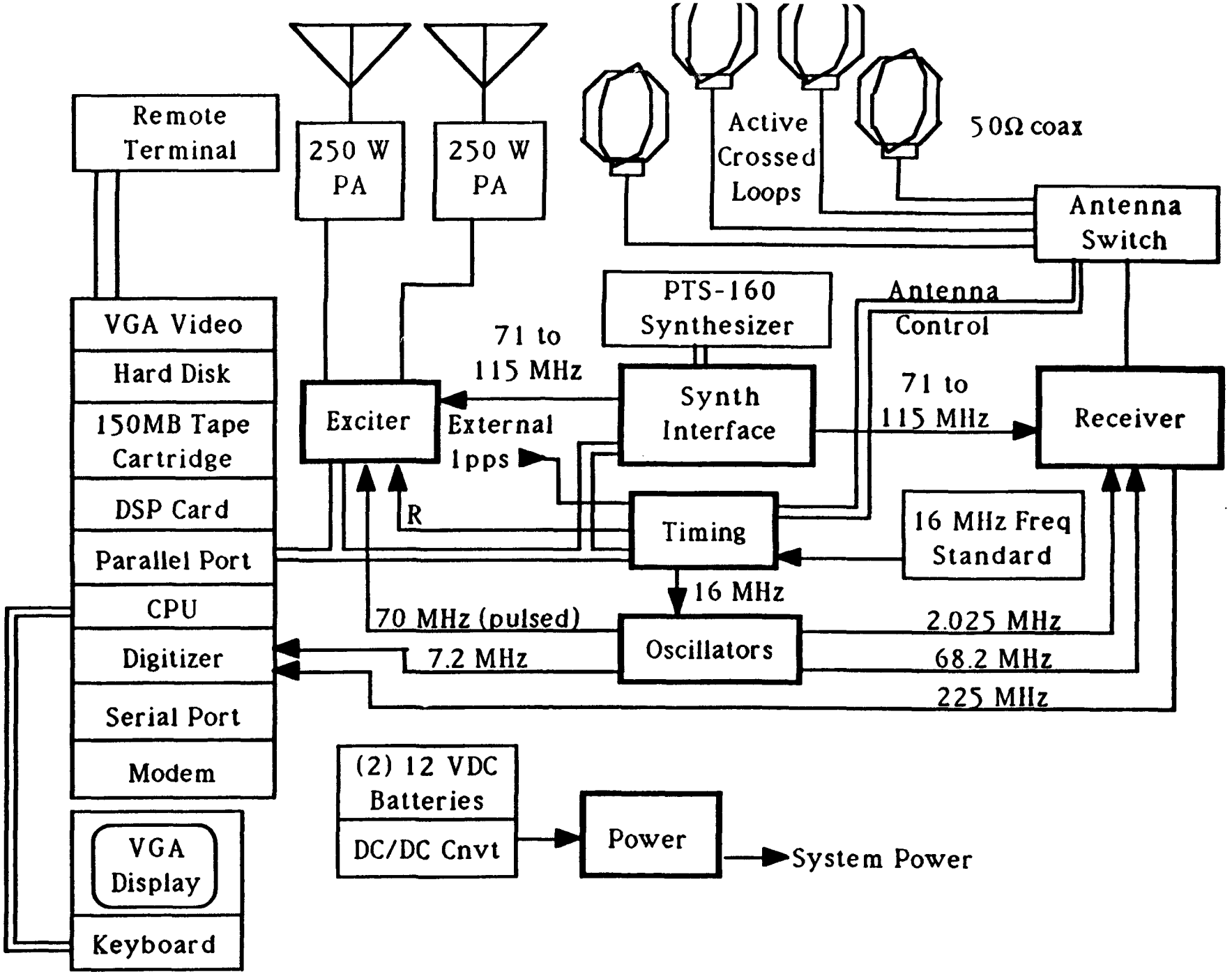

Figure 3. Digisonde Portable Sounder (S/N 01) System Diagram.

Because of the remote location of the Svalbard station it was determined that local retrofitting of the current system was not feasible. Therefore, a replacement DPS chassis was built and tested in November/December 1992. This replacement chassis was again hand-carried to Svalbard by Mr. Haines and Mr. Jurgen Buchau, Phillips Laboratory, in January 1993. The PTS synthesizer was removed and returned leaving an empty slot in the fiberglass enclosure unit.

Figure 4 presents the chassis layout of the upgraded chassis (system serial number 01A) and Figure 5 presents a system block diagram of the upgraded DPS architecture. Again in Figure 5 the blocks with a bold border, the Antenna Switch and Digitizer are circuit card assemblies designed by the ULCAR staff.

3.0 FIELD CAMPAIGNS

During the performance of the contract two field campaigns were conducted. The second campaign was combined with the DPS system upgrade.

3.1 Monitoring the Cusp Using the DPS

During the period 26 December 1991 through 12 January 1992 field campaign, Bodo Reinisch of ULCAR, and Jurgen Buchau of Phillips Laboratory, made DPS observations at Ny Alesund, Svalbard.

On arrival at the Svalbard station the DPS was fully operational. A few software changes were implemented into the DPS including an improved O/X recognition algorithm that Mr. Haines had judged unsatisfactory during system installation. The new software update resulted in excellent ionograms being output and recorded on cartridge tape. It was noticed, however, that the X-traces were weak and non-existent at low frequencies. The two coaxial cables feeding the two orthogonal transmit rhombic antennas were swapped resulting in neat O and X traces down to low frequencies. The output connectors on the rear panel of the transmitter chassis were labeled in ink to match the corresponding labels on the cables.

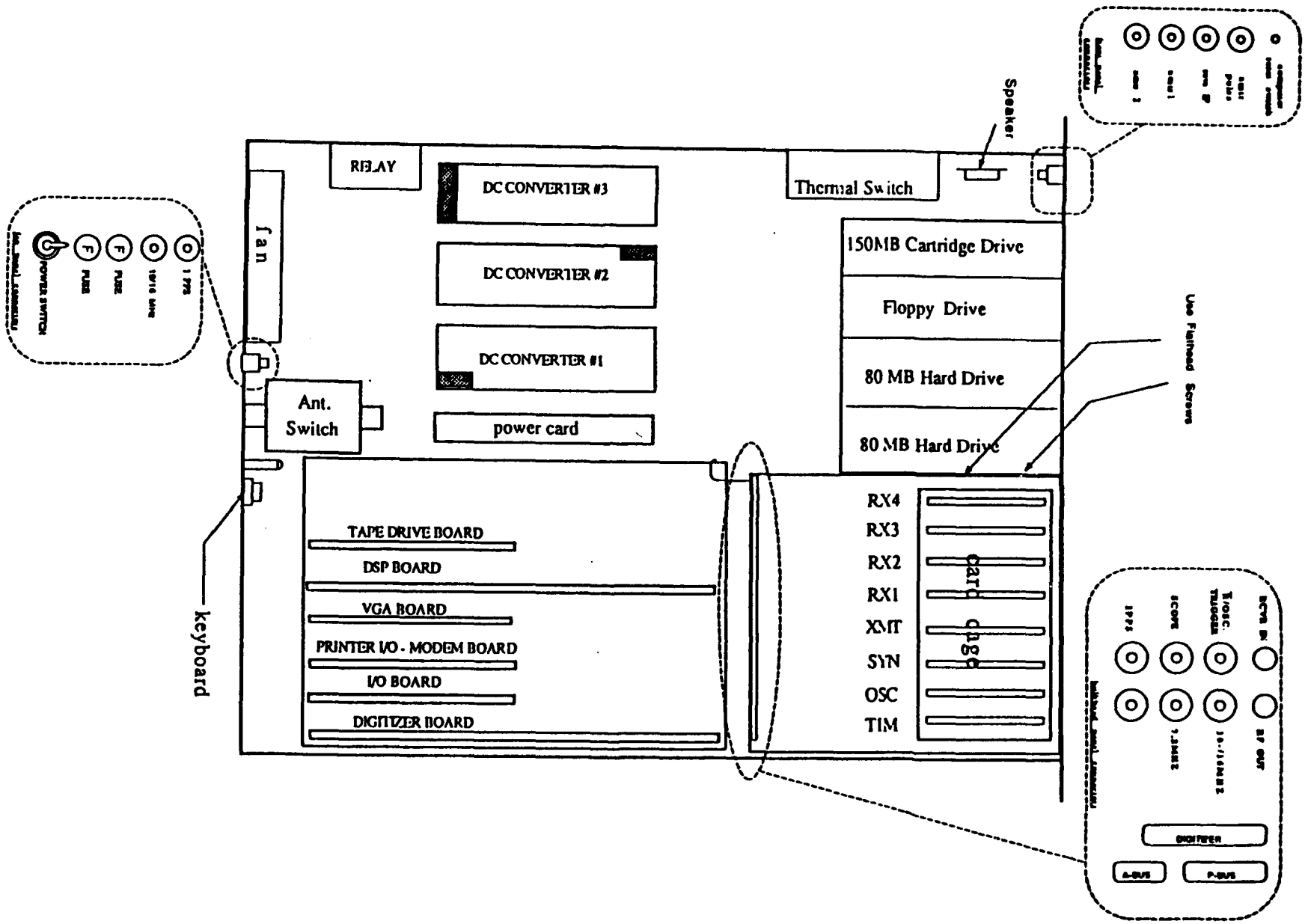

Figure 4. Digisonde Portable Sounder (S/N 01A) System Components.

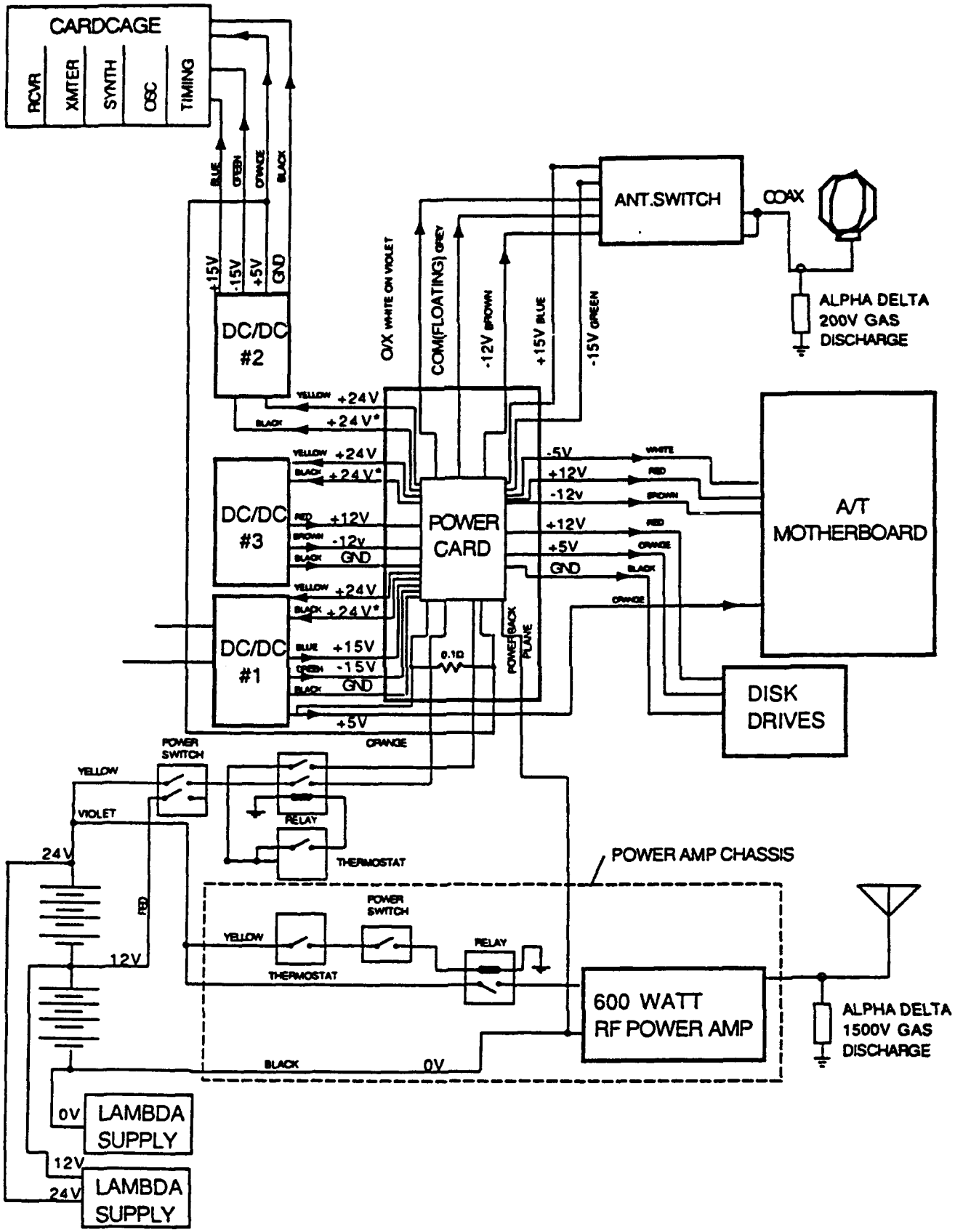

Figure 5. Digisonde Portable Sounder (S/N 01A) System Diagram.

Ionogram and drift measurements were made every five minutes. The ionograms measured Doppler (8 lines) and O/X polarization. Initially, drift measurements were made on 16 frequencies, spaced by 100 kHz, in 32 range bins each. Later this was reduced to 6 frequencies, spaced by 300 kHz, and 8 ranges. The spectra looked, in general, well behaved, although occasional overflow (aliasing) was observed. During a 24 hour period, the ionograms clearly show the entry of the station into the polar cap around 18 CGT (14:30 UT), when E and F1 ionizations disappear and the F echoes start to form well organized traces, indicating one, two or three main reflection areas. When patches arrived, foF2 increased sometimes to 11 MHz from background values of 3 to 5 MHz.

Around 06 CGT, the station enters the auroral region, and the ionograms show E and F1 ionization caused by precipitation. From 06 to 18 CGLT the ionograms generally look very turbulent. Without knowledge of cusp transition time, identity of the cusp from the ionograms could not be made.

3.2 DPS System Upgrade/January 1993 Campaign

In January 1993 Mark Haines accompanied Jurgen Buchau of GPI/PL to Ny Alesund to install and test the updated DPS and to collect ionogram and drift data.

Since the DPS system, installed in Ny Alesund in December 1991 was the first of the DPS sounders built there was a significant amount of improvement in the following year. We improved the stability of the transmitter power amplifier, the local oscillator sources, and the receiver's IF amplifier circuits as well as developing a custom digitizer card which greatly reduced the noise leaked into our received signal from other components in the DPS chassis (most notably the computer and power supplies). The major functional improvement was that the original DPS was not capable of detecting the angle of arrival of echoes in real time during the ionogram measurements. We call this capability beamforming since it is performed by digitally (or in the older Digisonde, the Digisonde 256, by analog delay lines) forming 8 independent beams in 7 different directions (6 azimuth directions and 2 overhead, one in left-hand circular polarization the other in right-hand circular polarization).

The required input data for the algorithm is a complex amplitude sample for each antenna resolvable height (typically each 5 km over a range of 90 to 730km) simultaneously sampled on each of the four receive antennas. The 1991 version of the DPS system could produce the raw data but the algorithm to select the input data (the same Doppler line value must be used on all four antennas), form the beams and detect the direction of signal arrival, plus the software to display and store this data in a meaningful way was only developed during 1992. It was tested extensively under laboratory conditions and at Millstone Hill in Westford, MA. The technique is to compute the phase delays as a function of antenna position (relative to the central antenna) which would be experienced by a wave arriving from the center of the beam direction, then use the complex conjugate of this phase delay as a weighting function to "correct" the phases of received signal samples such that when they are added, they will coherently sum for signals arriving in that direction and will coherently cancel (with only four antennas the cancellation is very rudimentary so maybe we should say they tend to cancel) for directions outside of the beam. The expression for such an operation is:

$$B_i(n) = \sum_{j=1}^{4} W_{ij}^{*} s_j(n)$$

where $B_i(n)$ represents the output signal for the ith beam as a function of time nT (where T equals the period between discrete samples), Wj is the complex weight (which "corrects" the phase of incoming signals) for data from antenna j and $s_j(n)$ is the received signal on antenna j as a function of time.

As mentioned earlier, the basic raw data was available in previous versions of the DPS-1 system but the selection, computation, display and storage software had to be developed and tested. The DPS produces a Doppler spectrum for each antenna at each height sample, whether there is one echo, many echoes or no echoes present at that range (the terms range, height and time delay are synonymous for vertical incidence sounding). Therefore, there are three classes of spectra which must be handled:

1. If one source is present in the signal from a given height there will be only one peak in the Doppler spectrum for that height, and it will be present in the same

position on all four antennas. In this case the complex amplitude of that one Doppler line is set aside in an output buffer in the DSP (digital signal processor) card from each of the four antennas. From here, the main computer is signaled when the output buffer is completed and it retrieves the data from the DSP and computes the beam amplitudes and declares a direction of arrival.

2. If no signal is present at a given height, the Doppler spectrum is filled with background noise and interfering signals which are often very strong and coherent signals from powerful radio transmitters. The noise signals are detected by the program running in the main computer such that they are thresholded out of the real time displays. However, no thresholding is applied to data stored on tape cartridges. Interfering signals, however, look very much like an echo to the computers and are therefore tagged with their correct direction of arrival, which is very seldom directly overhead. Therefore these off-vertical signals are ignored by the analysis programs and by human analysts for purposes of scaling the overhead ionosphere.

3. The most difficult situation is when more than one echo or echoes plus interfering signals appear in the Doppler spectrum at a given height.

   a. If they all have a different Doppler shift and the overhead DPS echo is the strongest signal on every antenna, then the correct Doppler sample will be placed in the output buffer.

   b. If there is some fading across the antenna array, one Doppler line could be strongest in one antenna and a different one in the others. In this case, since we select the one Doppler line position to be processed ONLY by analyzing antenna 1's Doppler spectrum, it is guaranteed that we will use the same Doppler line from all antennas.

   c. If the overhead signal is present in the Doppler spectrum but another signal is stronger, currently the program will ignore the desired overhead signal and select the stronger one, since the selection is currently done before the angle of arrivals are computed. We plan to enhance the DSP program such that in the future it will analyze several of the strongest signals and select the overhead signal if it is there. However, since the

Doppler resolution is so coarse in the beamforming ionogram mode, it is not clear that oblique signals can really be separated from overhead, so this remains to be seen.

d. If more than one signal is received in the same Doppler line, the phase of the line is corrupted, however, the beam corresponding to the stronger signal will have the stronger summed response, so the algorithm should make the correct direction determination.

Experimental Results in Svalbard

During the Ny Alesund Patches campaign in January 1993, we noticed that the beamforming mode produced an unusually high number of off-vertical echoes (as compared to mid-latitude results), especially just prior to magnetic noon (about 0900 UT). Since these errors occurred in the middle of traces which were clearly the overhead ionosphere, we attempted to improve the operation of the system.

The first step to trying to remedy this situation was to increase the accepted cone of vertical angles which would still be tagged as vertical from 15 to 22.5 degrees. This change only served to tag too many off-vertical traces as vertical, thus causing more errors.

The next step taken was to correct the phase shifting that occurs due to the sequential sampling of the 4 antennas from pulse to pulse. In the 10msec that passes between sampling of each antenna 1% of a cycle (2π radians) of phase change will occur for each 1Hz of Doppler shift in the received signal. Therefore the Doppler resolution must be computed at the beginning of each measurement and the resulting phase correction must be made for the 10, 20 and 30 msec which pass between the sampling of antennas 2, 3 and 4 respectively, to make the phase sampled on these consistent with the phase sampled on antenna 1. In mid-latitude ionospheres the motions are so slow that the resulting Doppler shift is insignificant, therefore this correction is only effective in these Arctic ionospheres. A noticeable improvement occurred after making this correction, but we were still not convinced that all the obliquely tagged echoes were truly off-vertical. However, since the phase correction was certainly one step in the right direction we left it in effect without attempting to quantify the resulting improvement.

The next step was to scan the Doppler spectrum for the maximum amplitude line from +1/4 of the Doppler range to +1/2 then back to -1/2 and up through 0Hz to +1/4. This has the effect of replacing a high Doppler maximum with one of lower Doppler shift in the case where they have the same amplitude. Since overhead echoes have less radial velocity than off-vertical echoes, this favors the overhead signals.

The next step was to change the time domain window function which prepares data records for Fourier transformation (computation of the Doppler spectrum uses an FFT algorithm). Our simulation program FEEDDSP4 clearly shows that a simple FFT algorithm which uses a Hanning (or any other) weighting function will produce spreading in the spectral domain and the adjacent lines over which the spreading occupies exhibit a π phase shift relative to its neighbors. We did not notice this phenomenon when using a Rectangular windowing function (all weights equal 1, i.e. no weighting) since the test signal is not spread at all and therefore there is no adjacent line to compare to the phase. However, this effect is present with the rectangular window just as it is with the Hanning window and can be seen when a signal spans two Doppler bins. Later, we discovered that this is a fundamental property of the FFT, not the windowing function.

Since the phase error phenomenon was markedly worse when Svalbard was in the magnetic noon sector we realized early on that our main problem may be that the high velocities characteristic of that environment were causing the Doppler shifts to wrap around the end of the Doppler spectrum and appear on the other side. This makes positively shifted signals appear negatively shifted. Since the Doppler dependent phase correction terms are only correct if the signals appear at their true Doppler line, the application of these correction terms to wrapped around signals just degrades them further.

The gray shaded ionograms in Figures 6 and 7 show the volatility of the beamforming algorithm to the extremely high Doppler conditions present in Svalbard. The ordinary polariation overhead echoes are displayed in black, the extraordinary echoes in gray (mainly frequencies above 4.4 MHz) and the off-zenith echoes in light gray. The ionogram in Figure 6 shows enough overhead O-echoes for ARTIST to determine a good F trace with a good foF2 value of 4.7 MHz, while the ionogram in Figure 7, only 10 minutes later, could not be scaled by ARTIST

because of the randomness of received phases as a function of antenna position was so severe that only a few F-layer trace points are presented as overhead. The gray shade ionogram in Figure 8 shows a typical example of the beamforming working perfectly at Svalbard with the light grey again indicating the off-vertical echoes. As long as the drift velocities are such as not to cause aliasing, resolution and accuracy of the ionograms are excellent. To overcome the problem with aliasing, the system needs to be expanded to a DPS4, so that 4 receivers can sample the four antennas simultaneously, thus increasing the sampling rate by a factor four.

4.0 SUMMARY OF SCIENTIFIC RESULTS

A DPS began continuous recording of ionospheric parameters and velocities at Ny Alesund (78.2°N, 15.7°E) in December 1991. The location of this station is important in mapping out the location of the reversal boundary of the convection boundary and in conjunction with stations like Qaanaaq, Greenland; Sondrestrom, Greenland; and College Station, Alaska will allow the large scale configuration of the polar convection pattern to be specified. The data gathered at Svalbard have already been beneficial in the interpretation of the movement of ionization across the polar cap when compared to data recorded at Qaanaaq and College Station. As an example of these comparisons let us look at a data set recorded during the period January 7 through 9, 1992.

Figure 9 shows the drift velocity components measured at Qaanaaq during the period January 7 through 9, 1992. This figure displays the horizontal velocity magnitude (v_h), the vertical velocity magnitude (v_z) and the azimuth (A_z) of the drift direction. The azimuthal values are represented by the scattered points and error bars in the lower panel of Figure 9. The continuous line in this plot represents the antisunward direction that is expected at this station for these particular days. From previous statistics [Cannon et al., 1991] it is possible to make a prediction of the orientation of the IMF from these velocity components. During days 7 and 8, these data clearly displays drifts characteristic of Bz<0 and By<0. However, on day 9 a sunward motion is clearly observed indicating that the IMF Bz component reversed direction at 09 UT, i.e. Bz>0.

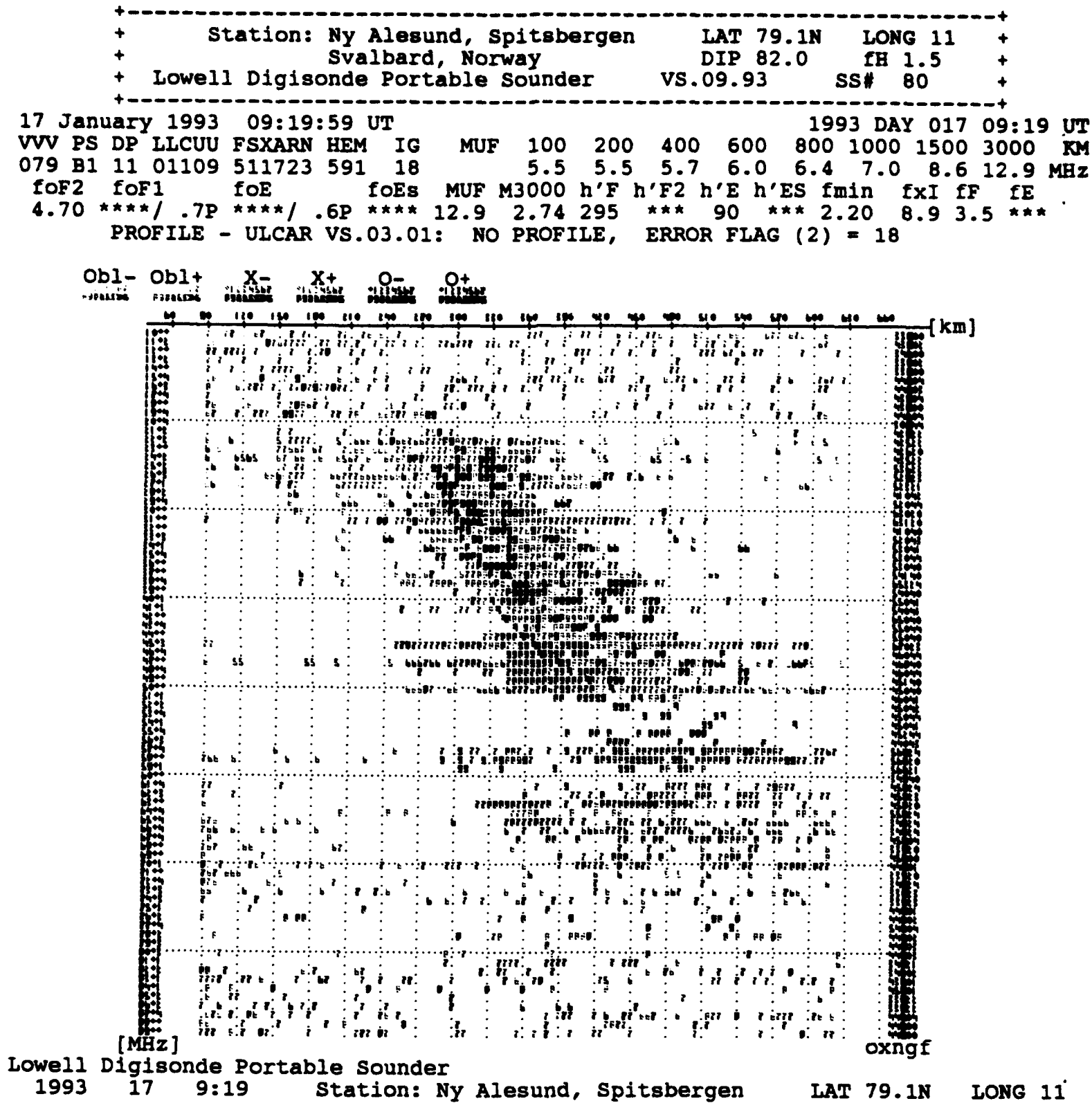

Figure 6. Beamforming ionogram showing amplitude and correctly scaled foF2 value; Svalbard Digisonde Portable Sounder; day 017, 0939 UT.

```
+------------------------------------------------------------------+
+      Station: Ny Alesund, Spitsbergen      LAT 79.1N   LONG 11   +
+               Svalbard, Norway             DIP 82.0    fH 1.5    +
+  Lowell Digisonde Portable Sounder      VS.09.93      SS#  80     +
+------------------------------------------------------------------+
17 January 1993  09:29:59 UT                          1993 DAY 017 09:29 UT
VVV PS DP LLCUU FSXARN HEM  IG   MUF  100  200  400  600  800 1000 1500 3000  KM
079 B1 11 01109 511723 591  18       5.4  5.4  5.6  5.9  6.3  6.9  8.6 12.9 MHz
 foF2  foF1     foE       foEs  MUF M3000 h'F h'F2 h'E h'ES fmin  fxI fF  fE
 4.60 ****/ .8P ****/ .6P  2.4 12.9  2.81 255  ***  90  108 1.40  8.9 3.6 ***
      PROFILE - ULCAR VS.03.01:  NO PROFILE,  ERROR FLAG (2) = 18
```

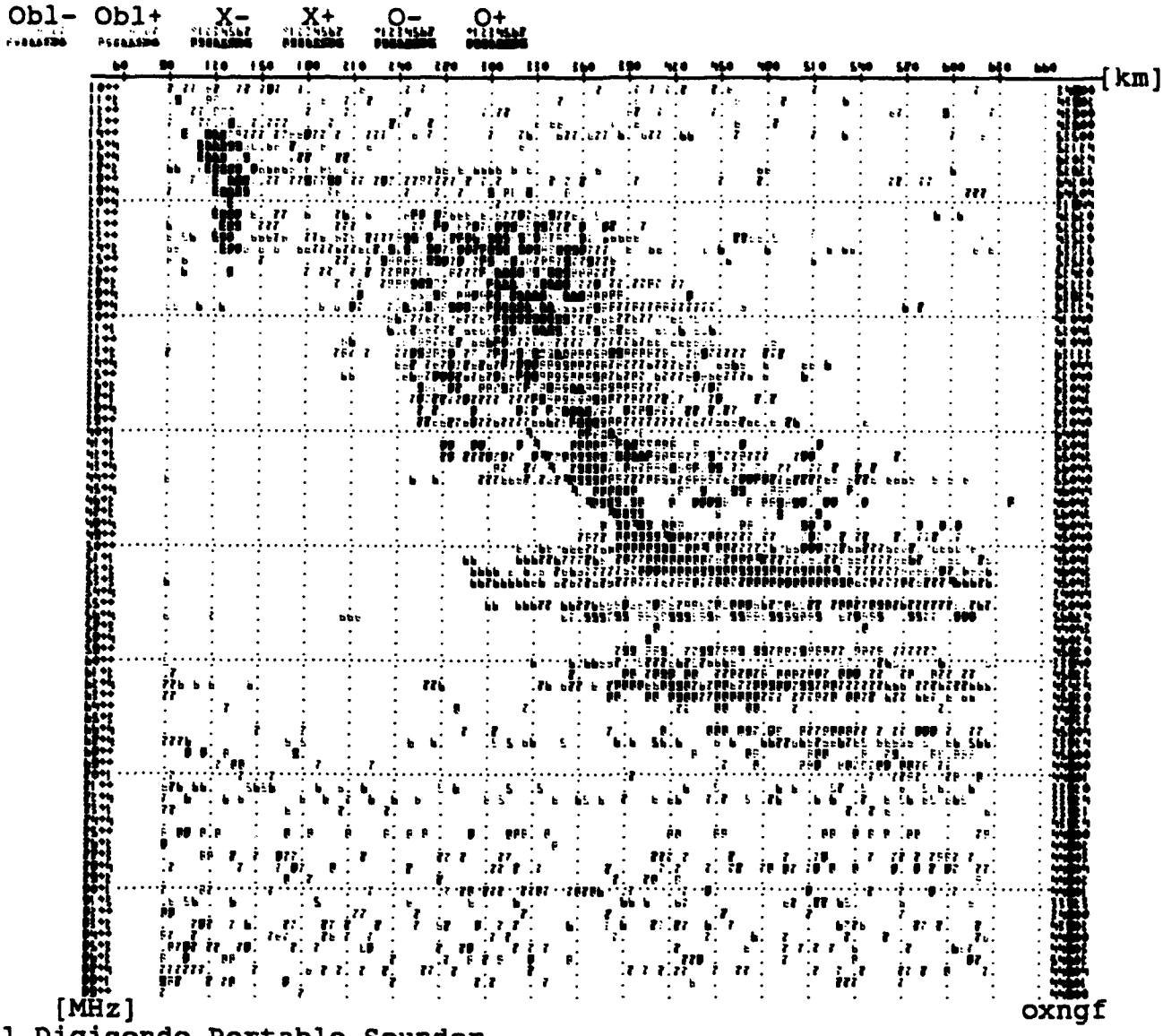


```
Lowell Digisonde Portable Sounder
  1993   17   9:29      Station: Ny Alesund, Spitsbergen      LAT 79.1N   LONG 11
```

Figure 7. Beamforming ionogram showing randomness of received phases as a function of antenna position; Svalbard Digisonde Portable Sounder; Day 017, 0929 UT.

```
+------------------------------------------------------------------+
+    Station: Ny Alesund, Spitsbergen   LAT 79.1N  LONG 11.9E      +
+               Svalbard, Norway        DIP 82.0   fH 1.5 MHz     +
+  Lowell Digisonde Portable Sounder     VS.04.93     SS#  80      +
+------------------------------------------------------------------+
10 May 1993  21:00:59 UT                                  1993 DAY 130 21:00 UT
PS DP LLCUU FSXARN HEM  IG       MUF  100  200  400  600  800 1000 1500 3000  KM
B2 10 01111 511724 591  18            5.4  5.4  5.6  6.0  6.5  7.2  9.2 14.5 MHz
 foF2  foF1     foE       foEs  MUF M3000 h'F h'F2 h'E h'ES fmin  fxI fF   fE
 4.60 ****/4.1P 2.00/2.0P 2.00 14.5  3.15 240  *** 105  105 1.20  6.7 1.4   .2
      PROFILE - ULCAR vs.02.01
         W =    .0  KM
         FSTART PEAK HT   A0       A1       A2       A3       A4     DEV   ROOTS
          [MHZ]  [KM]     [KM]     [KM]     [KM]     [KM]     [KM]   [KM]/PT
      E    .200 101.855 -31.506   3.734   6.283                        4.7    1
      F1
      F2  2.010 240.766 -98.703 -25.319  -1.318  -1.868   -.774   3.3    -
```

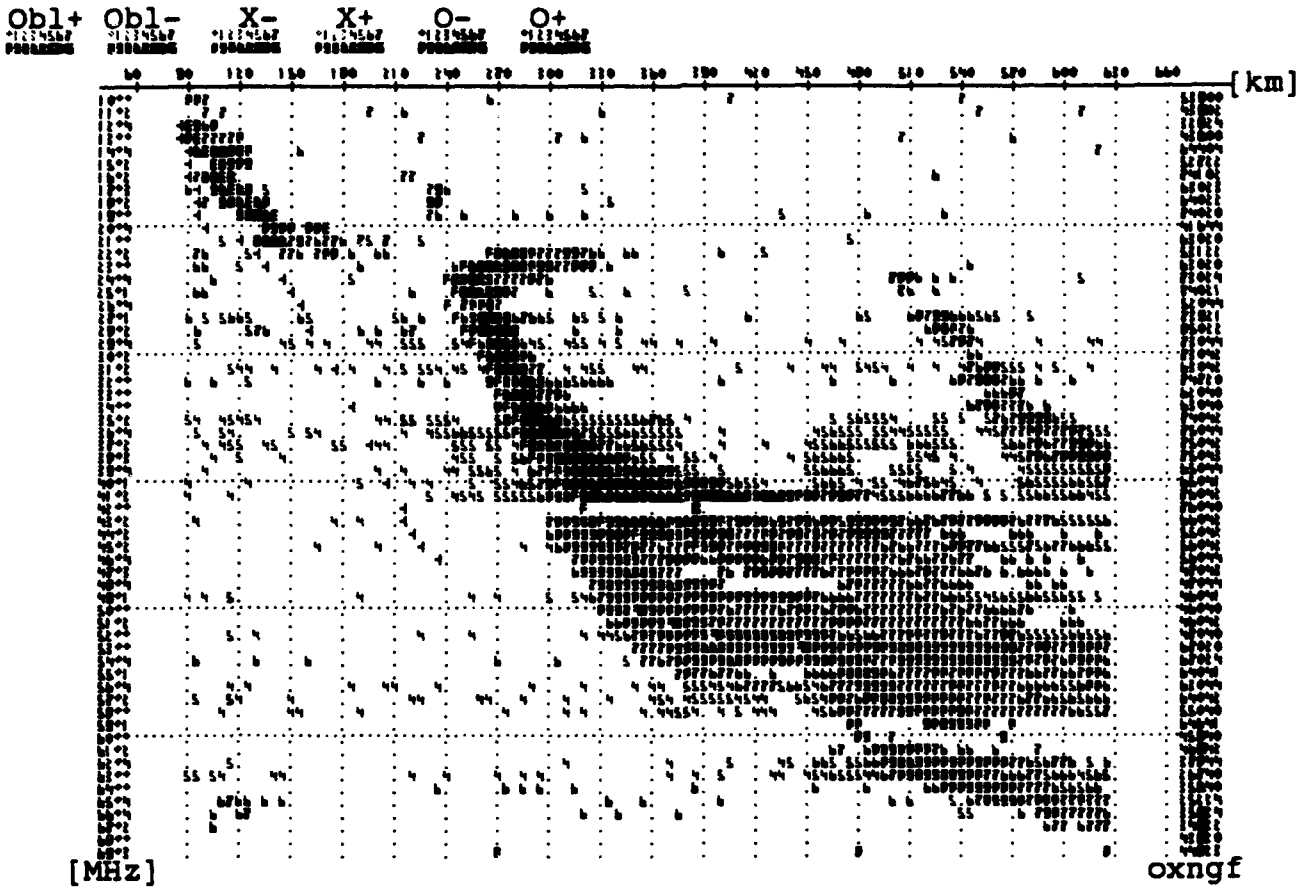


```
Lowell Digisonde Portable Sounder
  1993  130  21: 0   Station: Ny Alesund, Spitsbergen   LAT 79.1N  LONG 11.9E
```

Figure 8. Beamforming ionogram showing good beamforming technique; Ny Alesund Digisonde Portable Sounder, Day 130, 2100 UT.

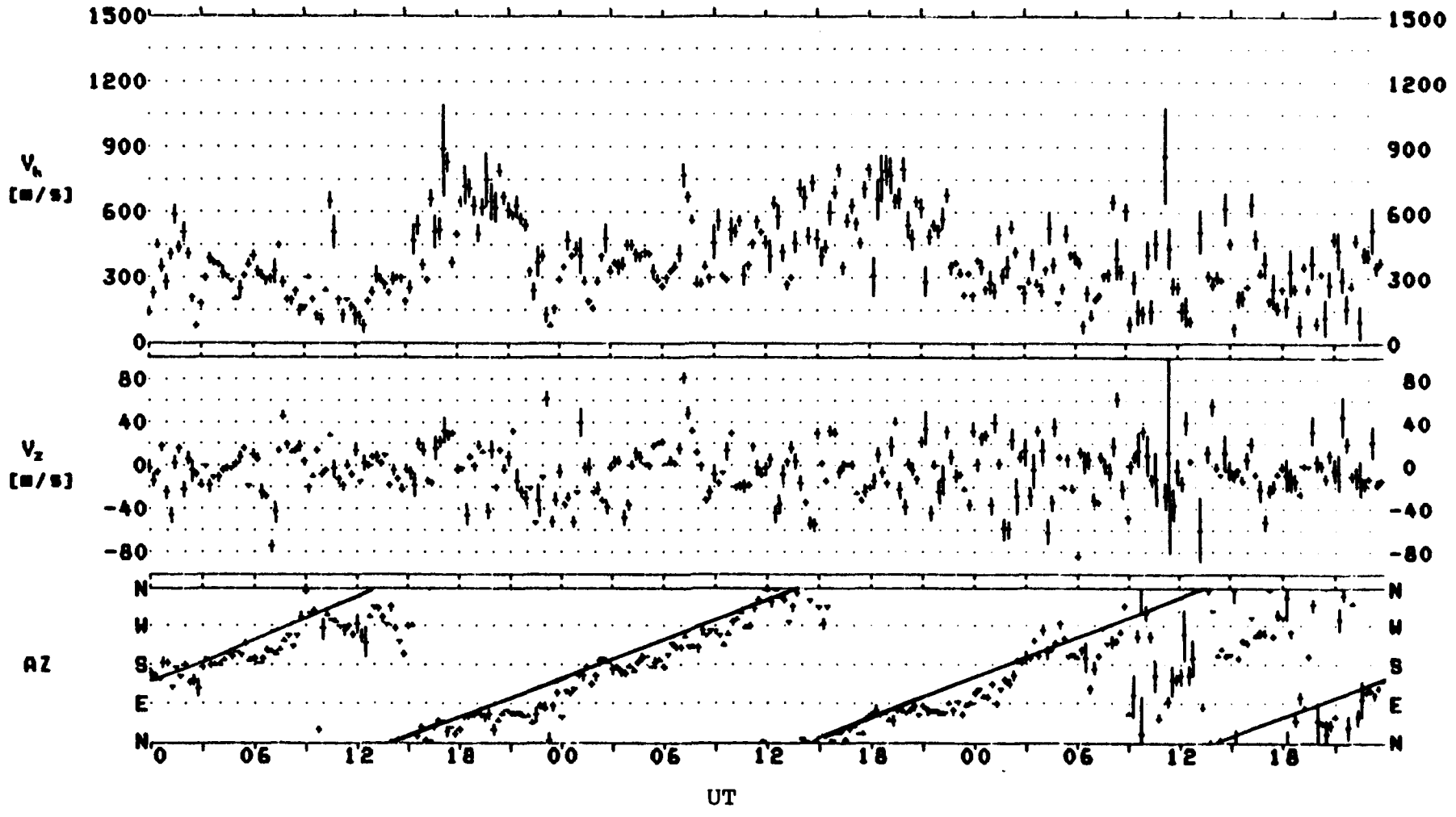

Figure 9. Horizontal, vertical and azimuthal velocity components for Digisonde 256, Qaanaaq, Greenland, for the period 7 - 9 January 1992.

Figures 10, 11 and 12 show the critical frequencies (foF2) observed at Svalbard, Qaanaaq, and College Station for January 6 through 8, 1992. Characteristically, at College Station, which is located at a geographic latitude of 65°N, there is the consistent diurnal variation with high foF2 values during the daytime and low values at night. This behavior is not observed at the two higher latitude stations, Qaanaaq (76°N geographic) and Svalbard (75°N geographic) which are in darkness for 24 hours. Distinct enhancements in foF2 at Qaanaaq and Svalbard can be associated with the movement of "patches" of enhanced electron densities across the polar cap [Buchau et al., 1988; Buchau and Reinisch, 1991]. At College Station, the electron densities begin to increase at about 19 UT reaching values well over 11 MHz. This produces a reservoir of ionization which when reached by the convection cells can send patches into and across the dark polar cap. The enhancement in foF2 starting around local noon at Qaanaaq (Figure 11) are not the direct result of solar irradiation [Buchau et al., 1988], but the result of convection which carries the daytime ionization from the sunlit North American sector (Yellowknife) across the polar cap. This is illustrated in Figure 13 which shows the noon-to-midnight line for Ny Alesund through the corrected geomagnetic pole at 2030 UT, i.e. at 0000 CGLT at Ny Alesund. This midnight meridian intersects the sunlit subauroral ionosphere at about 1400 LSOT. Although College Station is further west by three hours, we use it here to obtain an estimate of the electron densities, or foF2 values, for this local time. Figure 12 shows critical frequencies larger than 10 MHz from 10 - 17 LSOT, or 17 - 24 UT at Yellowknife. If we assume the Heppner and Maynard (1987) flow pattern for Bz<0 and By<0 (Figure 14) we see that the Yellowknife - College Station region is in the sub-cusp zone when Ny Alesund is at magnetic local midnight (2030 UT). Qaanaaq at this time is in the high speed dusk sector (18 CGLT). The density of the flux lines in Figure 14 is proportional to the convection speed, and suggests high speeds at Qaanaaq from 15 to 21 CGLT, or 1630 to 2230 UT. This is in good agreement with the velocities v_h observed at Qaanaaq on days 7 and 8 (Figure 9) showing velocities above 500m/s. When Qaanaaq is at 14 CGLT (1530 UT) it is in the best position to start observing patches transported at high velocities from the cusp at 09 CGLT. The middle and lower panels (days 7 and 8) in Figure 11 indeed show a group of intense patches arriving at 1630 UT on 7 January and 1800 UT on 8 January. The approximate travel time from the sub-cusp region to Qaanaaq for a velocity of 0.5 km/s would be a little more than one hour. Ny Alesund records patches starting a little later, at 1900 UT

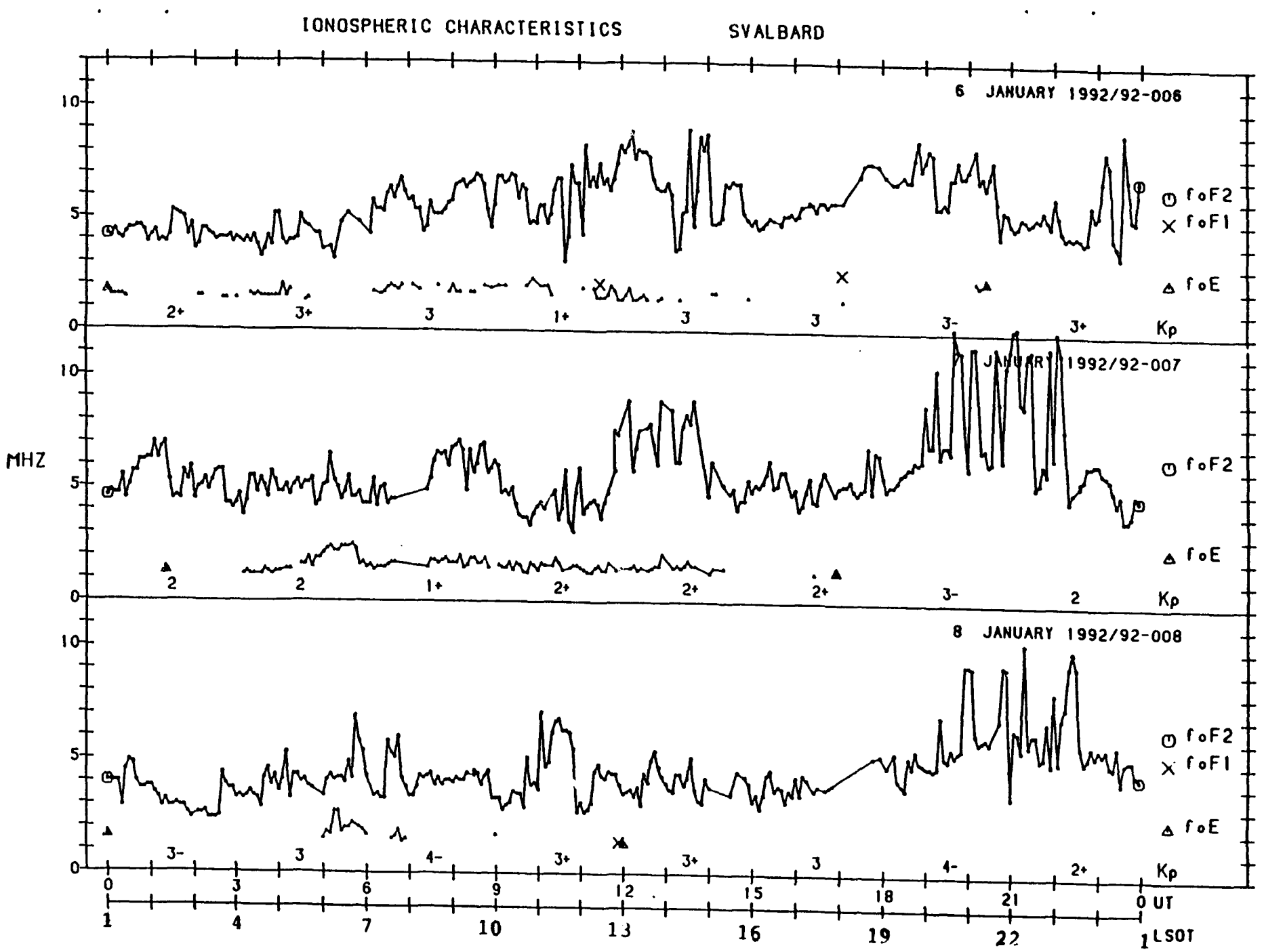

Figure 10. Critical frequencies (foF2) observed using the Digisonde Portable Sounder at Svalbard for the period 6 - 8 January 1992.

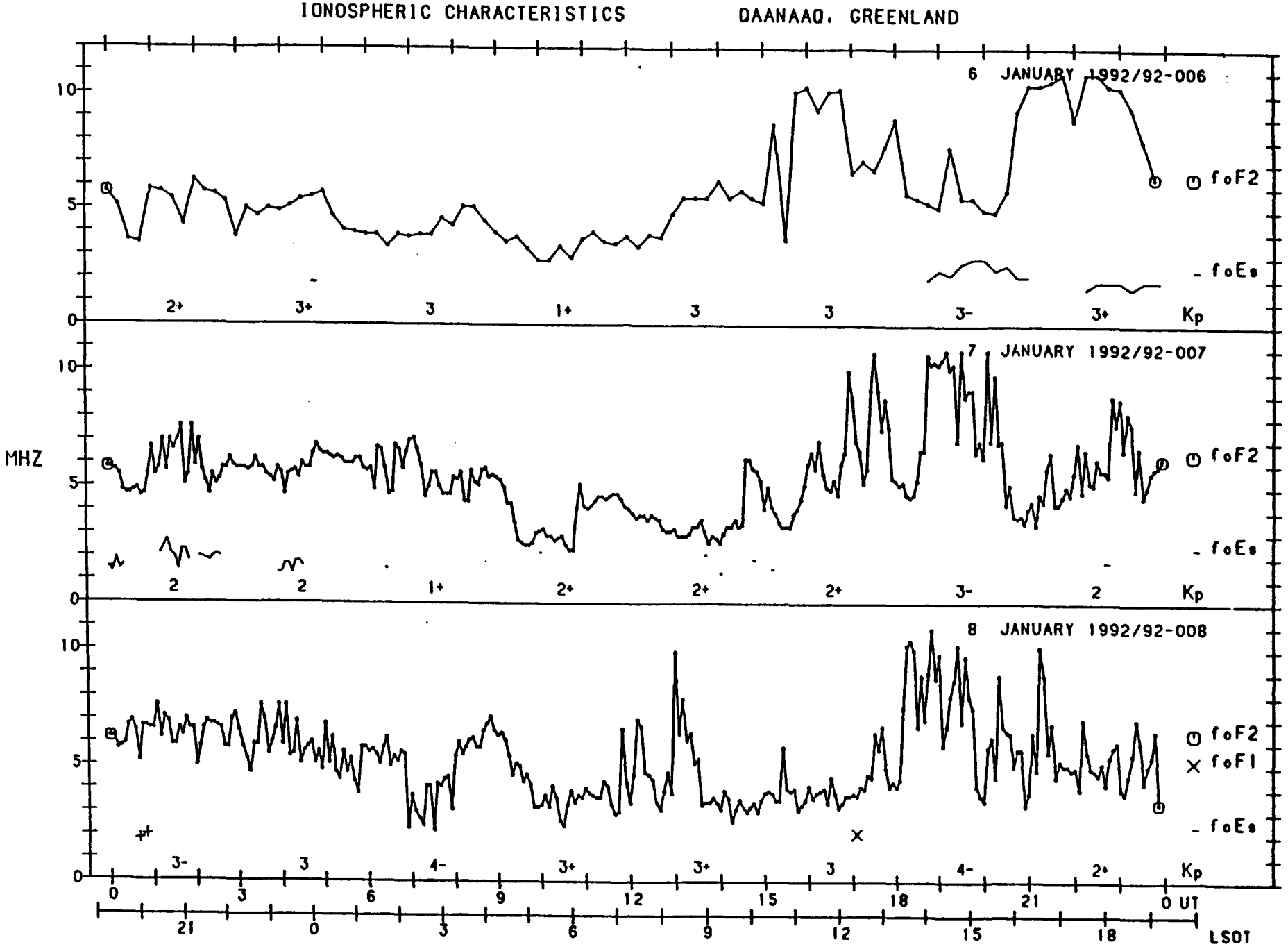

Figure 11. Critical frequencies (foF2) observed using the Digisonde 256 at Qaanaaq for the period 6 - 8 January 1992.

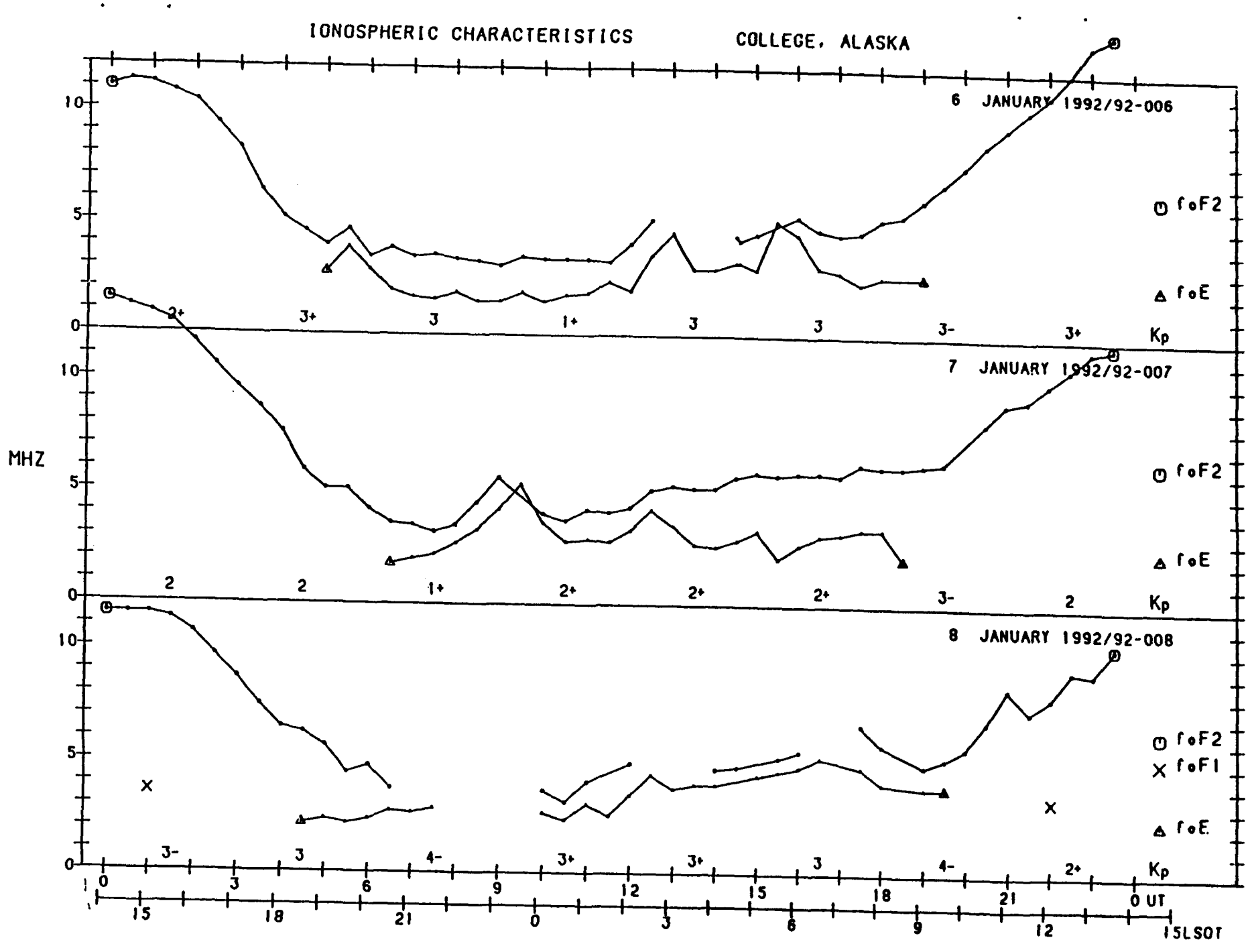

Figure 12. Critical frequencies (foF2) observed using the Digisonde 256 at College Station for the period 6 - 8 January 1992.

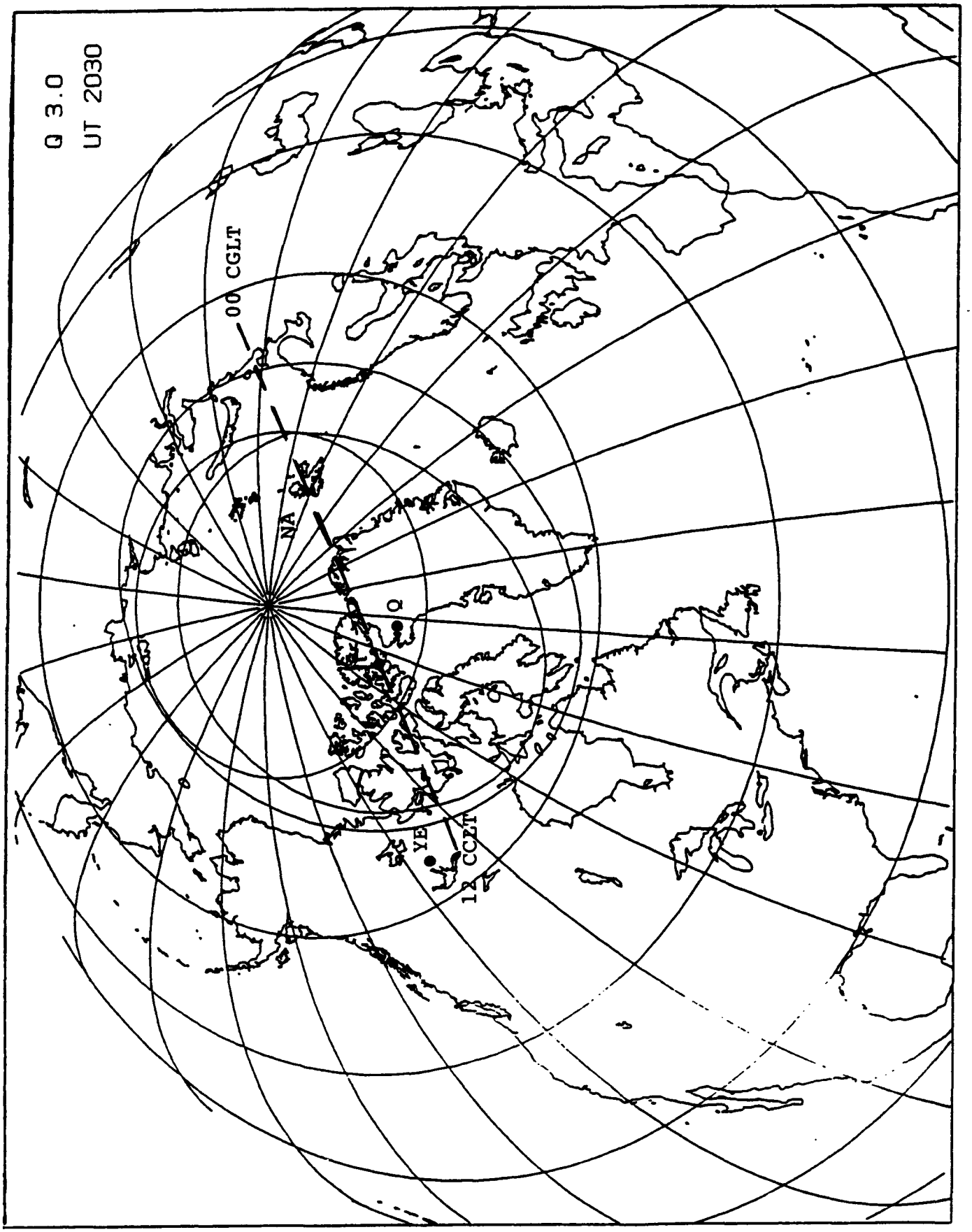

Figure 13. Magnetic midnight meridian for Ny Alesund.

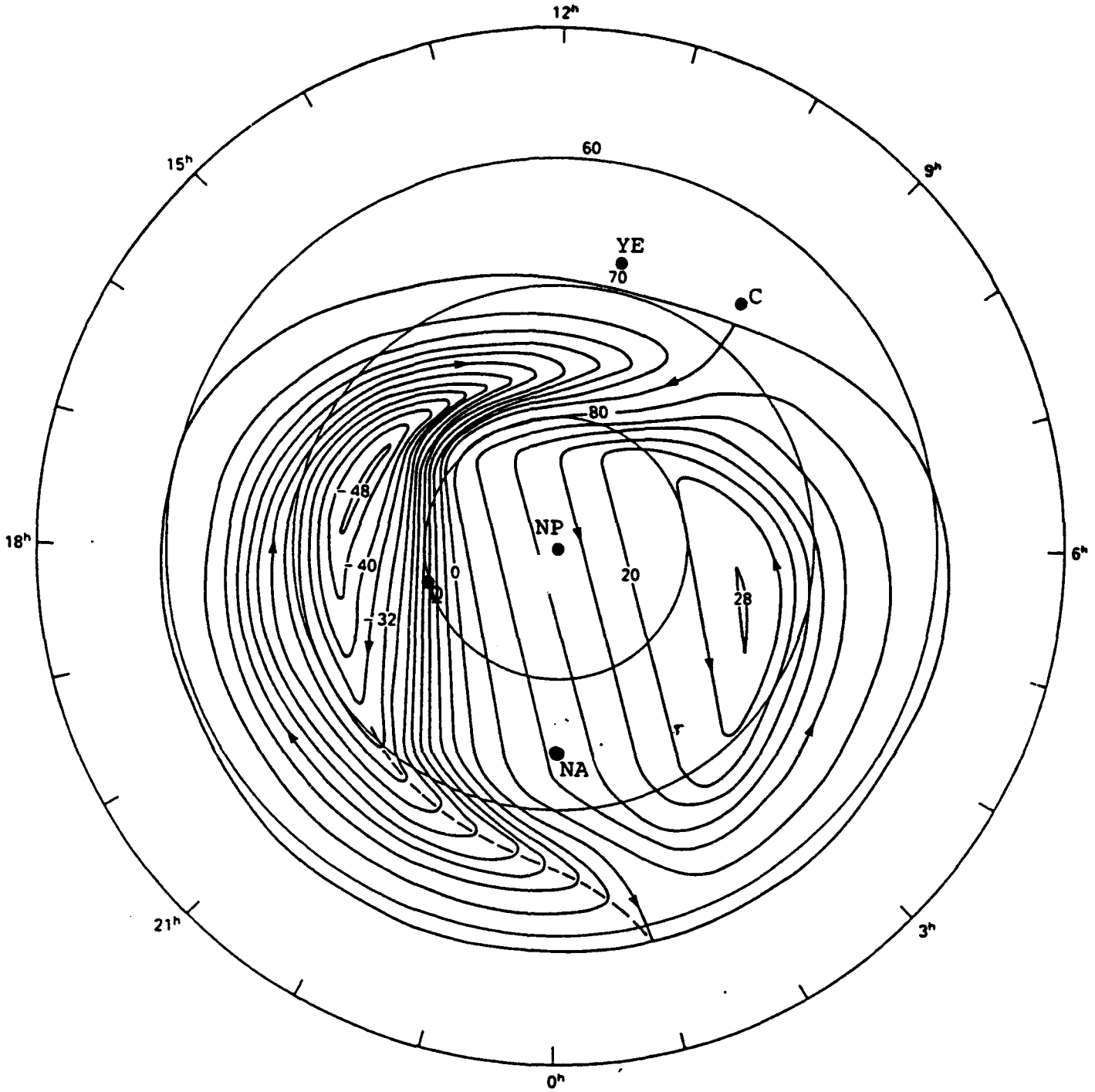

NA - Ny Ålesund
Q - Qaanaag
YE - Yellowknife
C - College
NP - Corr. Geom. North Pole

Figure 14. Convection pattern for Bz<0, By<0, after Heppner and Maynard (1987).

and 1930 UT, respectively, or 2230 CGLT and 2300 CGLT. The Ny Alesund patches are not necessarily the same, or at least not all of the ionization as observed at Qaanaaq. It seems that Ny Alesund sees the intense patches when it enters the high speed region (see Figure 14). Judging from Figure 14 we can expect a travel time between 30 - 50 minutes from Qaanaaq to Ny Alesund for a velocity of 500m/s. This would mean that a patch group at Qaanaaq seen at 1845 UT is the one seen at Ny Alesund at 1920 UT on day 7. Because of the multiplicity of patches it is difficult to identify individual patches, but the general process of transport across the pole to Ny Alesund is very convincingly demonstrated by the data.

The movements of ionospheric patches or irregularities over Svalbard produce at times distinct signatures in the ionograms. Figure 15 shows one such ionogram recorded on 5 March 1993, 1515 UT. The optifont numbers represent echo status (O, X, Doppler and angle of arrival). In this example, the vertically returned O and X spread echoes (7 and 15 for O, band 14 for X) are clearly identified and separated. In addition, two off vertical echo regions are identifiable. One echo trace at 230km is represented by number font 5 indicating negative Doppler shifts for echoes from the E-NE direction. The more noticeable off-vertical echo, located at a virtual height of 350 km, has an optifont character of 13 indicating positive Doppler shift. The consistency of this second off-vertical echo trace over a long frequency range indicates that the reflection surface of the irregularity is large scale and located some distance away from the station. As previously mentioned, the DPS was alternating between ionogram and drift observations. In Figure 15 four shaded boxes illustrate those frequencies and height ranges sampled by the DPS for the drift analysis. In this case four frequencies were probed and for each frequency spectra, 128 spectrum lines were recorded for 16 ranges separated by 10km.

The selected drift mode allowed the simultaneous sampling of the overhead ionosphere and the oblique irregularities. For each height-frequency bin the complex spectrum of each antenna signal is recorded. Figure 16 displays the Doppler spectra recorded for a frequency of 2.9 MHz and height of 290 km. The amplitude (on the left) and phase (on the right) spectra are shown for the 4 antennas in the lower part of Figure 16. The spectral amplitude distribution has a most probable value (MPV) of 22dB. This value is used as the noise threshold.

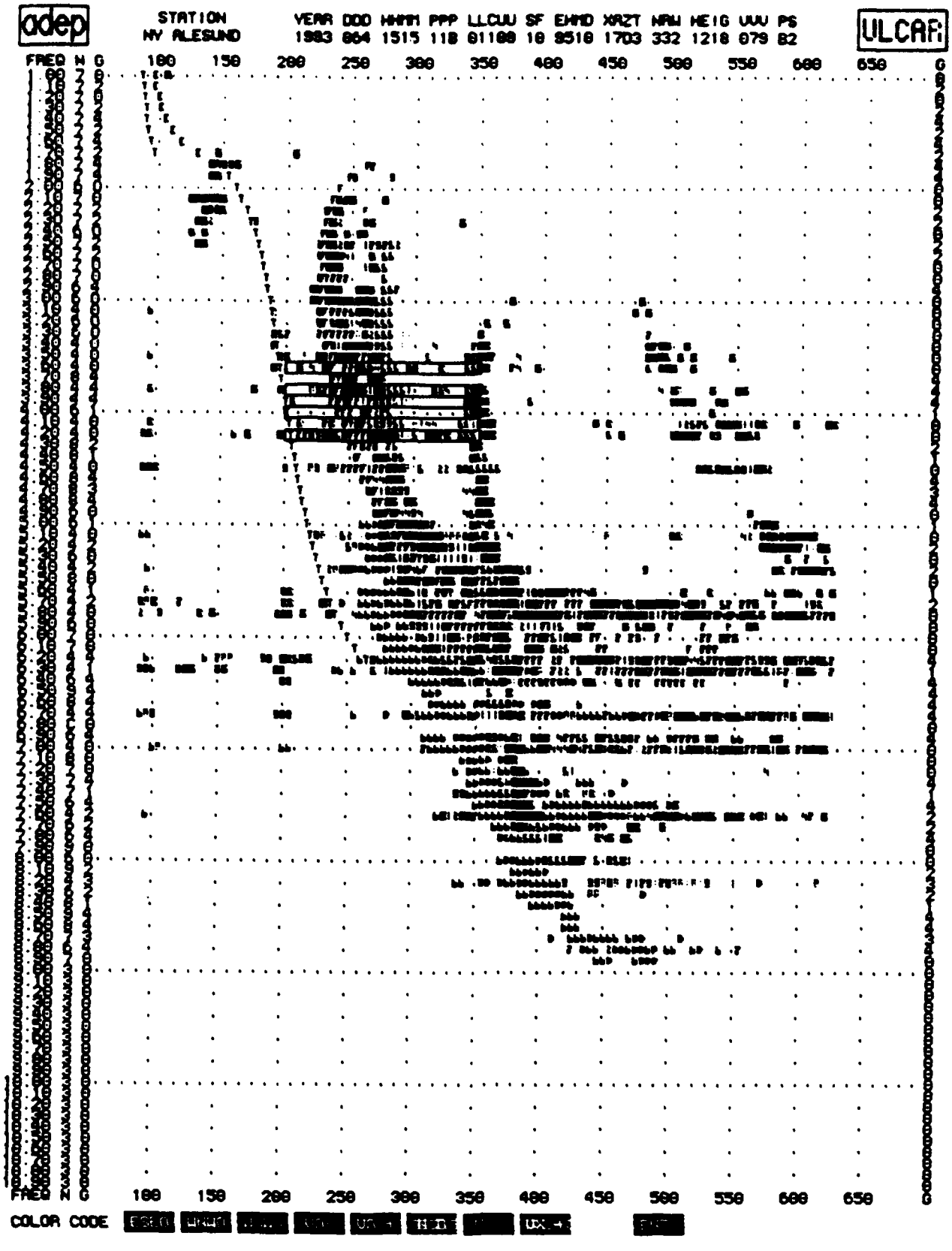

Figure 15. Digisonde ionogram recorded at 1515 UT on 5 March 1993. Darker shaded boxes display height and frequency ranges for drift measurement.

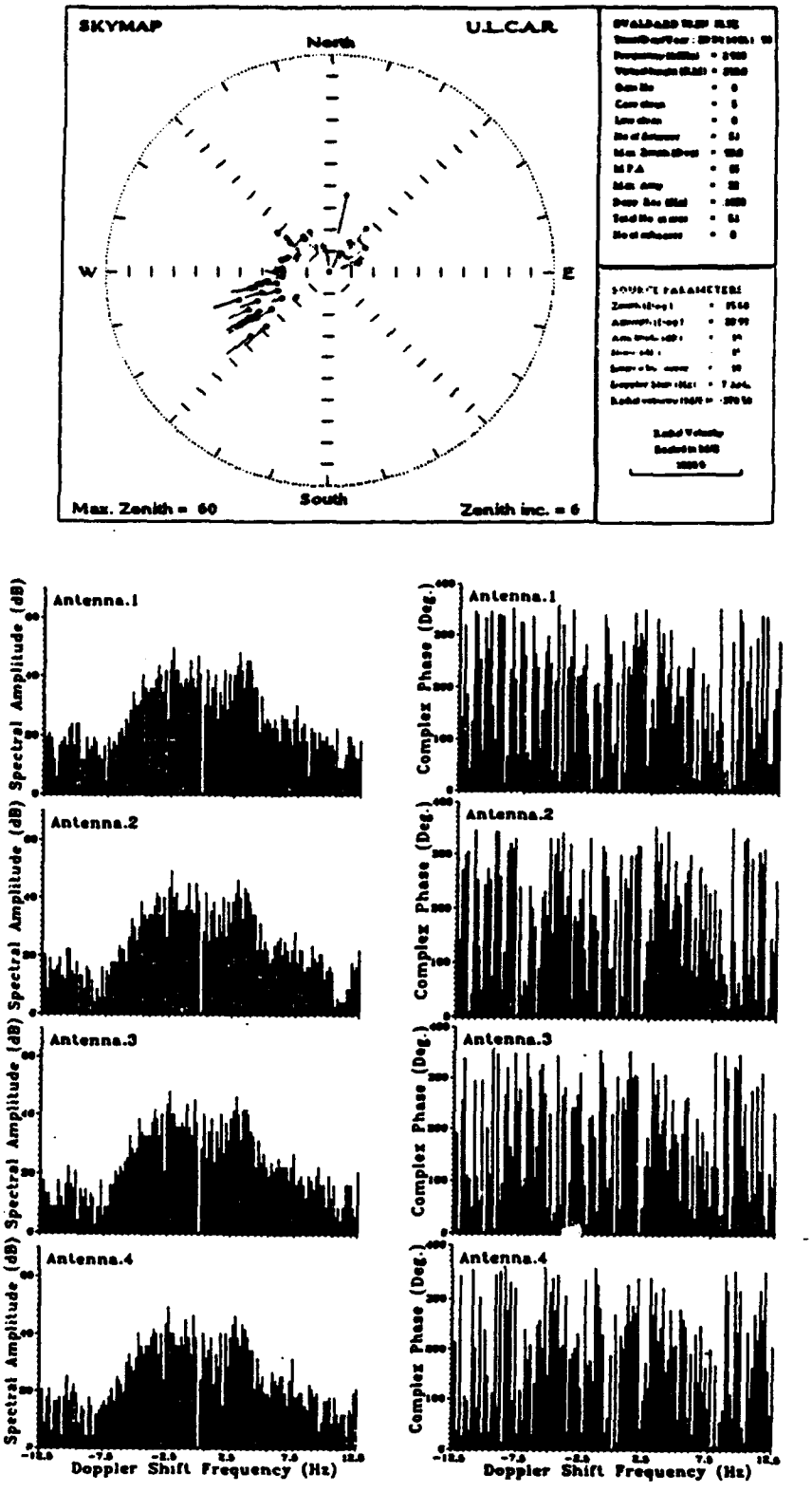

Figure 16. Plots of echo location points for radio waves reflected from the ionosphere (i.e. Skymap), and the complex amplitude and phase spectra used in calculating these points.

Spectral lines with amplitudes greater than the MPV are considered sources and for each Doppler line, using the phase differences between the four antenna signals and carrying out a least squares fit, the reflection source position is determined. These source position points are plotted in the skymap on top of Figure 16. Hence, for the spectra given, 51 sources were located. Sources with lines pointing towards the center of the plot indicate reflection surfaces moving towards the station (i.e. positive Doppler) and the length of the line is a measure of the radial velocity. Sources tagged with lines pointing away from the center of the plot represent reflection surfaces moving away from the station (i.e. negative Doppler shifts). Such skymap plots gives a good account of the structure of the ionosphere for a particular electron density.

The skymaps in Figure 17 represent different drift data range intervals for sounding frequencies 3.6, 3.8, 4.0 and 4.2 MHz recorded immediately after the ionogram shown in Figure 15. Figure 17a shows the sources observed at virtual heights between 230 and 250 km. The ionogram in Figure 15 shows these echoes as coming from overhead. The high resolution skymap shows that most of these echoes are returned from a spread of zenith angles up to 12°. In Figure 17b reflection points calculated between height ranges of 270 to 290 km are displayed. The first off-vertical echoes in the ionogram are contained within this height range. The sources on the skymap are located in an anular ring between zenith angles of 18° and 30°. Figure 17c displays the sources for ranges of 330 to 350 km, where the strongest off-vertical trace is observed in Figure 15 in an E-NE direction. This data set confirms the added ability for the DPS drift analysis technique to identify specific reflection regions and to determine the velocities associated with the movement of each separate structure. The skymaps also illustrate that at some ranges echoes are received from all directions in a stressed ionosphere. The ionogram selects only the strongest echoes for display and is therefore not able to completely analyze the ionospheric structure.

The consistent monitoring of the movement of ionization in the high latitude region via the Digisonde ionogram and drift methods supplies important information needed to describe the structure of the convection pattern. The DPS at Svalbard proves a vital link to this system. Since December 1991 this station has been recording the ionospheric behavior. This in turn will lead to a better

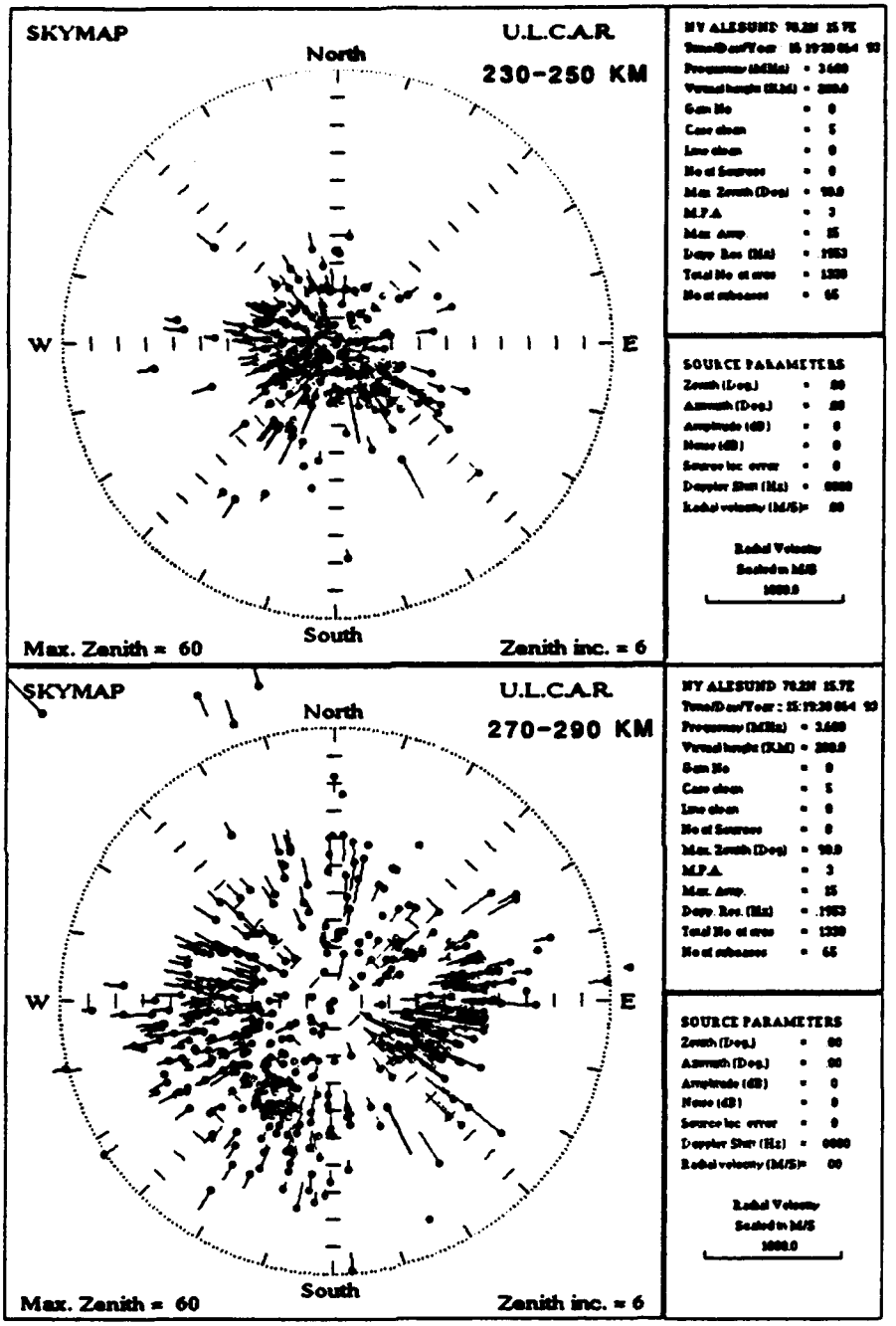

Figure 17. Skymaps displaying some reflection points calculated for data recorded at 1519 UT on 5 March 1993.

(a) Displays reflection points for radio waves returned within a virtual range of 230-250km.

(b) Displays reflection points for radio waves returned within a virtual range of 270-290km.

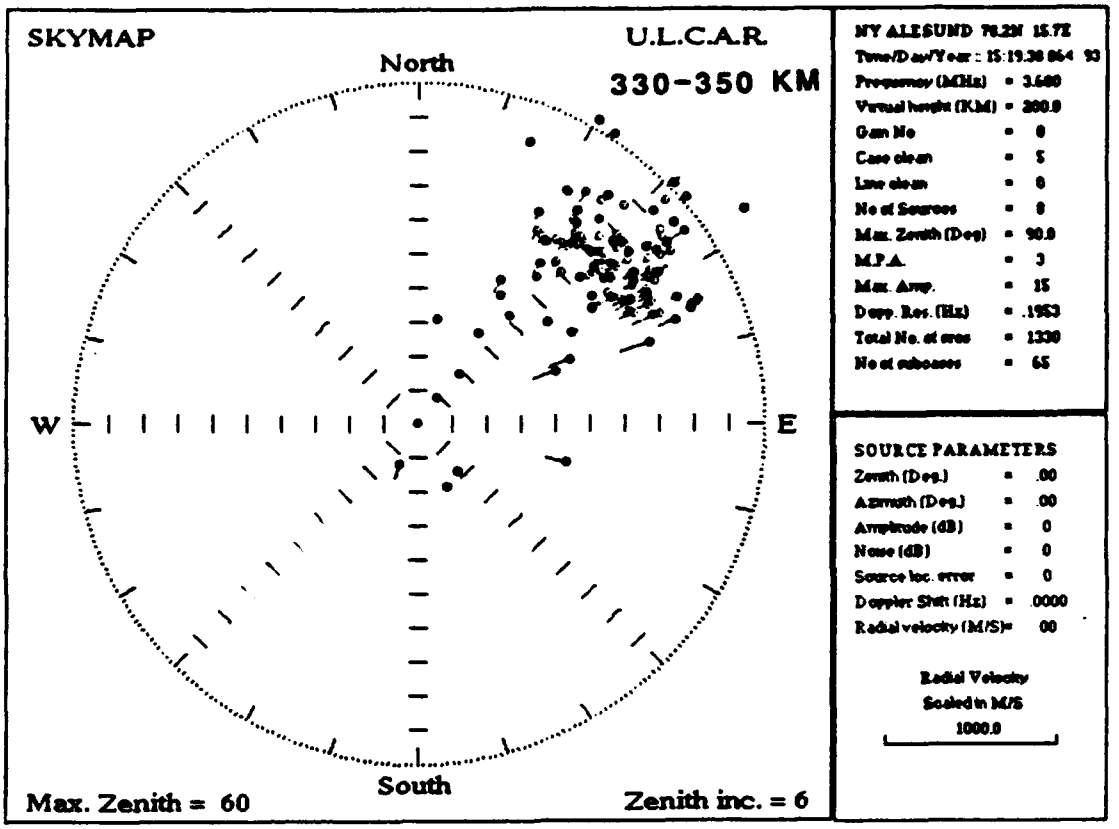

Figure 17. Skymaps displaying some reflection points calculated for data recorded at 1519 UT on 5 March 1993.

(c) Displays reflection points for radio waves returned within a virtual range of 330-350km.

understanding of the variability of the reversal boundaries. The plasma flow direction expected for Ny Alesund for Bz south condition is sketched in Figure 18 as a function of time [Buchau, 1992]. Anti-sunward flow is expected from 18 to 09 CGLT, 1430 to 0230 UT. During daytime hours from 09 to 18 CGLT the movement from one cell to the other in the cusp region introduces a jump in the flow direction from magnetic east to magnetic west.

Figures 19 to 23 display the v_z, v_h and A_z for Svalbard, March 2 through 6 (days 61 to 65), 1993. During this time the geomagnetic field was moderately disturbed with ΣKp from 16 to 35. The drift direction on day 61 is approximately antisunward from 17 to 24 UT as expected for Bz south. The Qaanaaq observations for this day (Figure 26) suggest Bz<0. The switch over from eastward to westward drift occurs at 13 UT (1630 CGLT). This would suggest a small dusk cell, i.e. By<0, which agrees with the Qaanaaq observations. The interpretation of the drift spectra during this transition period as the station moves from one cell to the next requires special attention. At these times the plasma flow may be quite large and radial velocities may not be supported within the -12 to 12 Hz Doppler shift range available. This tends to alias the spectra and introduce errors in the analysis technique as shown in Figure 24. Figure 24 displays the amplitude spectra for frequency-height combinations recorded from 1015 UT to 1045 UT on day 061 1993. In the first 31 samples recorded, the spectra are aliased as indicated by the large peaks observed at 13 Hz Doppler shift. After this time the spectra show smaller ionospheric movements that are contained well within the spectral range of the DPS system. Limited by the spectral range of the DPS the cusp region can be identified, however the data must be interrogated in detail at these times to assure that the calculated velocities are correct.

On day 62 (Figure 20) an eastward drift prevails from 0900 to 1630 UT(1230 to 2000 CGLT). Actually this means that the drift is almost antisunward from 11 to 14 UT (1430 to 1730 CGLT), as illustrated in the polar presentation in Figure 25a. The Qaanaaq data (Figure 26) indicate again Bz<0 for this day except perhaps around 15 UT when the Qaanaaq velocities are very small.

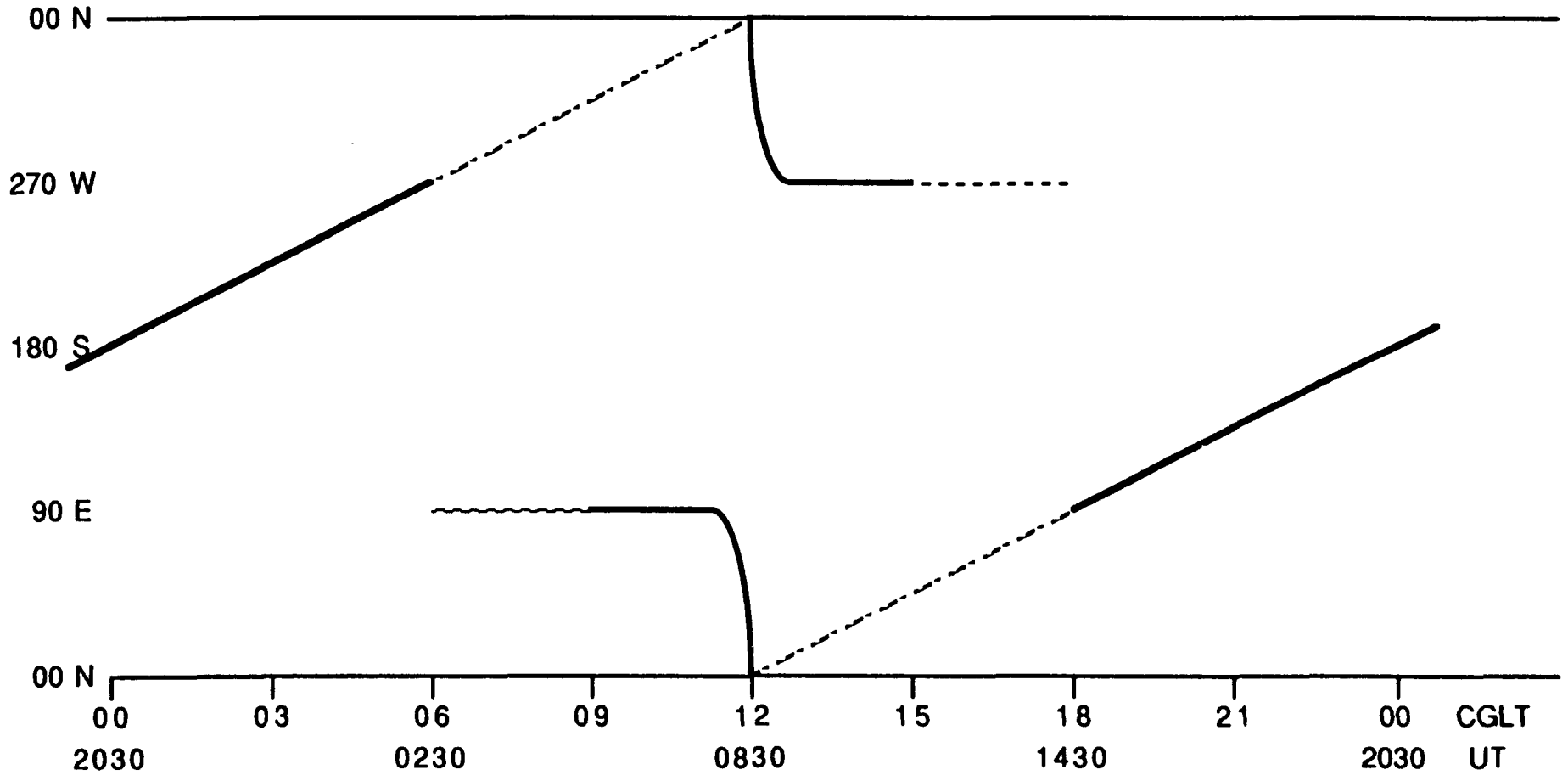

Figure 18. Expected flow direction at Svalbard (given in corrected geomagnetic coordinates) for simple symmetric two cell convection model for Svalbard.

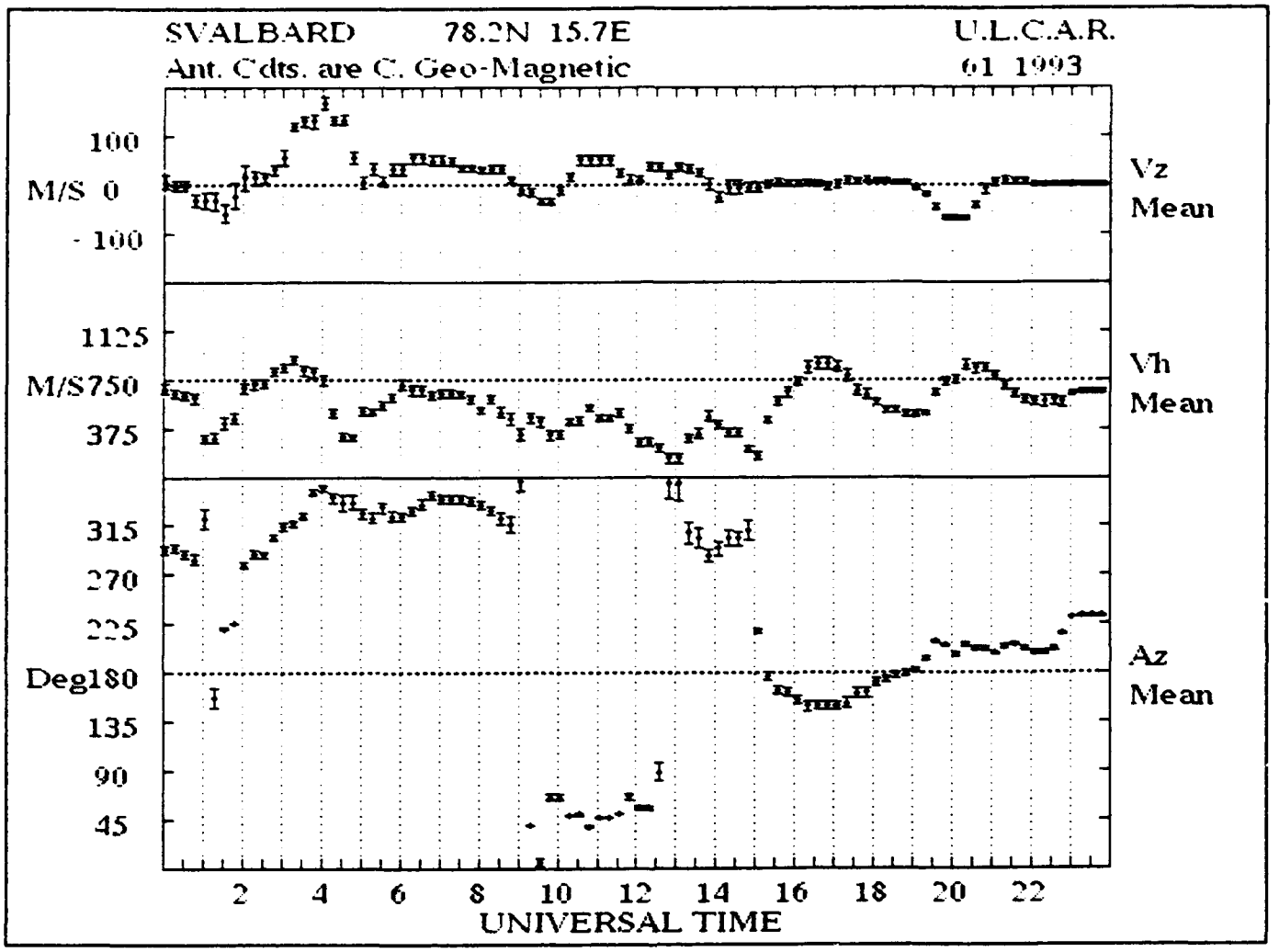

Figure 19. F region drift observed with the Digisonde Portable Sounder at Svalbard on 2 March 1992 (day 61).

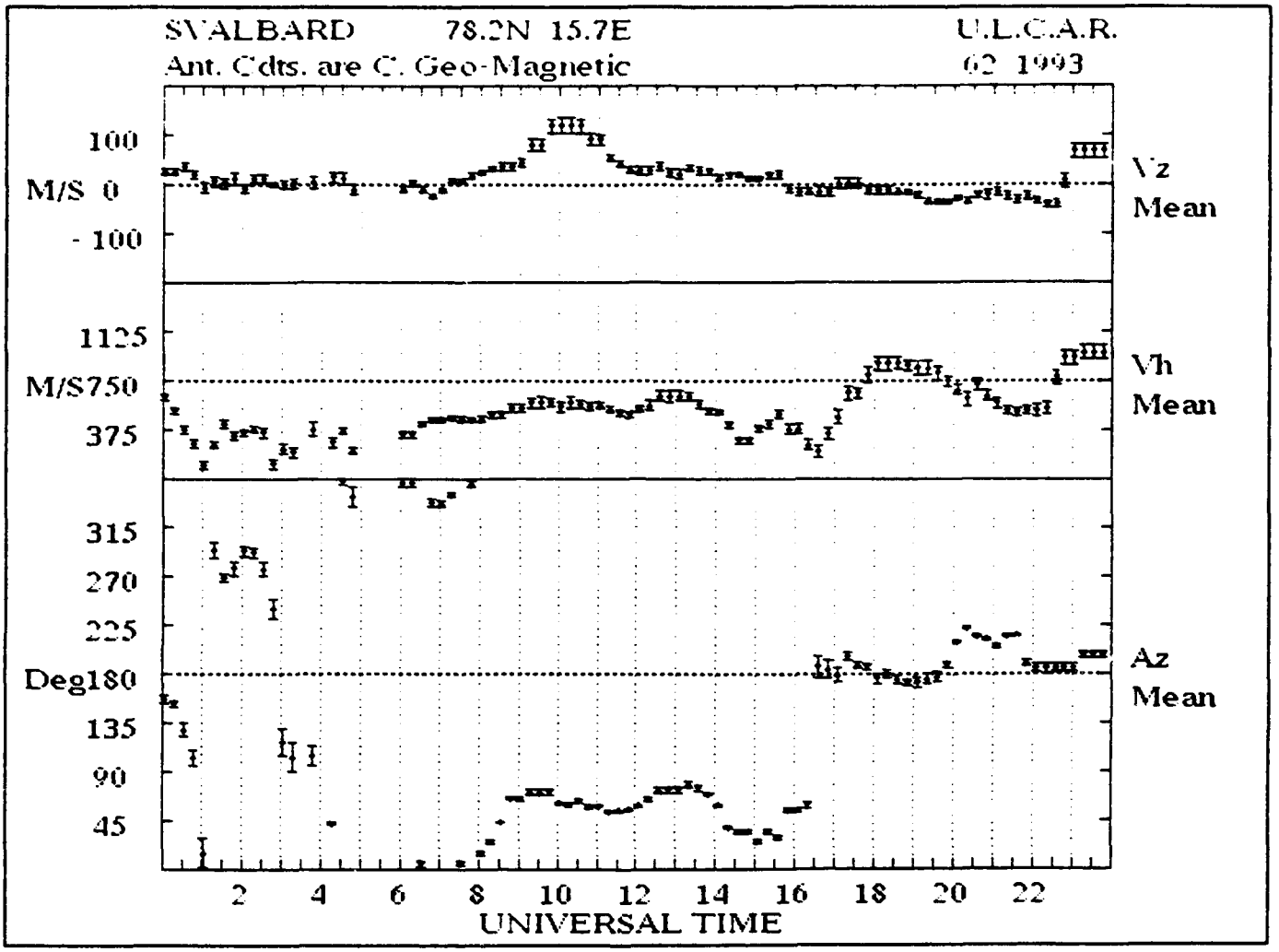

Figure 20. F region drift observed with the Digisonde Portable Sounder at Svalbard on 3 March 1992 (day 62).

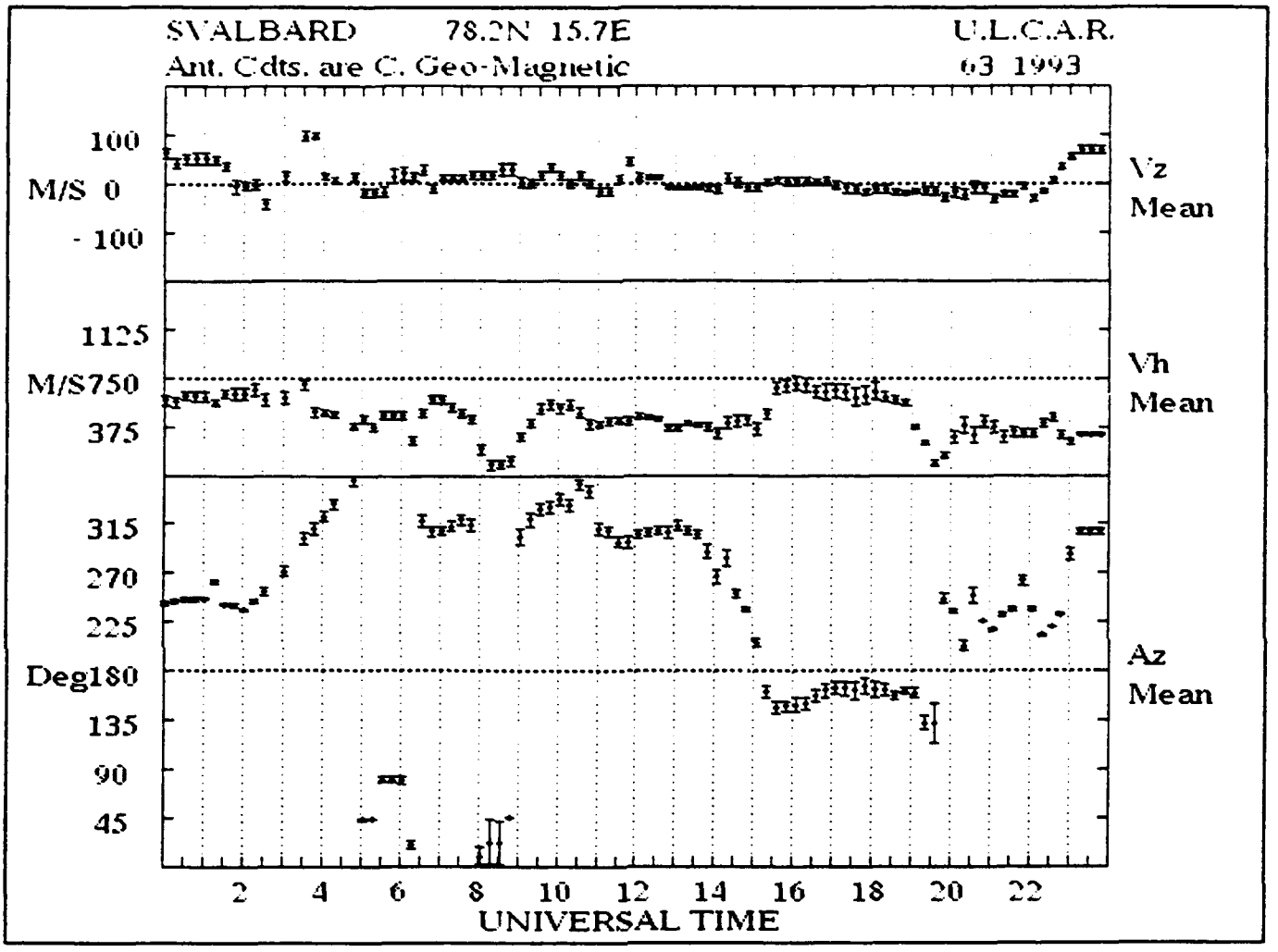

Figure 21. F region drift observed with the Digisonde Portable Sounder at Svalbard on 4 March 1992 (day 63).

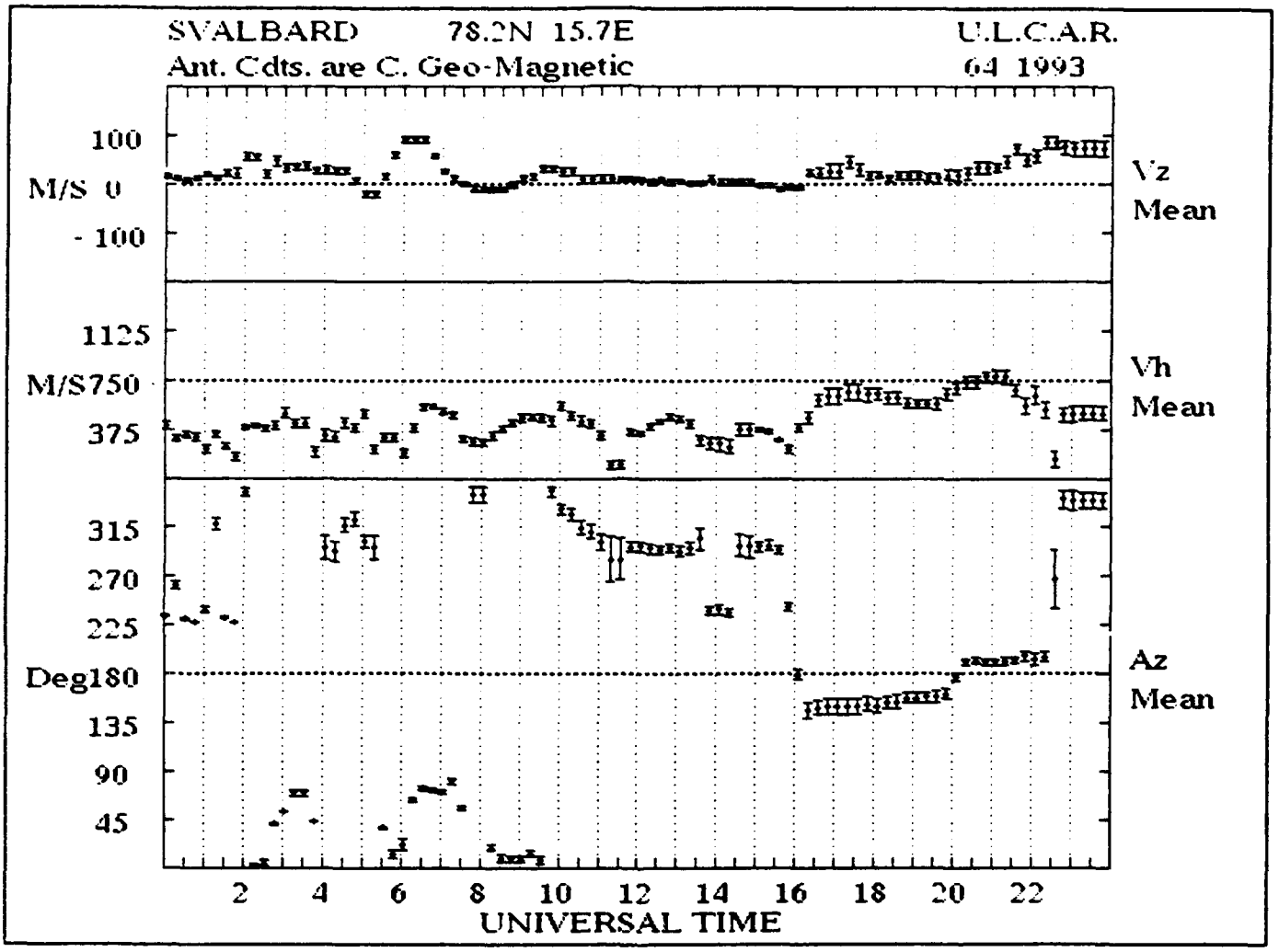

Figure 22. F region drift observed with the Digisonde Portable Sounder at Svalbard on 5 March 1992 (day 64).

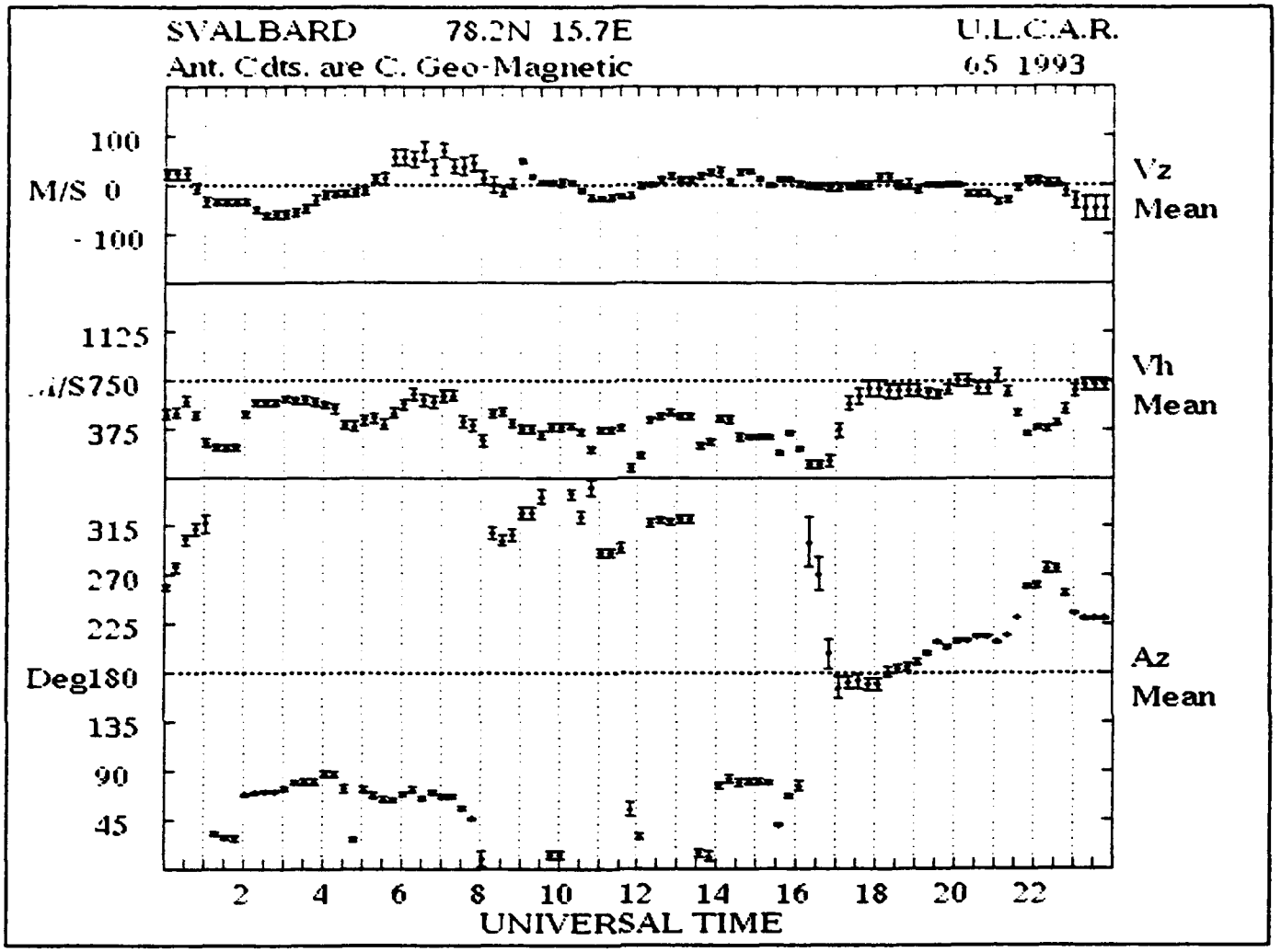

Figure 23. F region drift observed with the Digisonde Portable Sounder at Svalbard on 6 March 1992 (day 65).

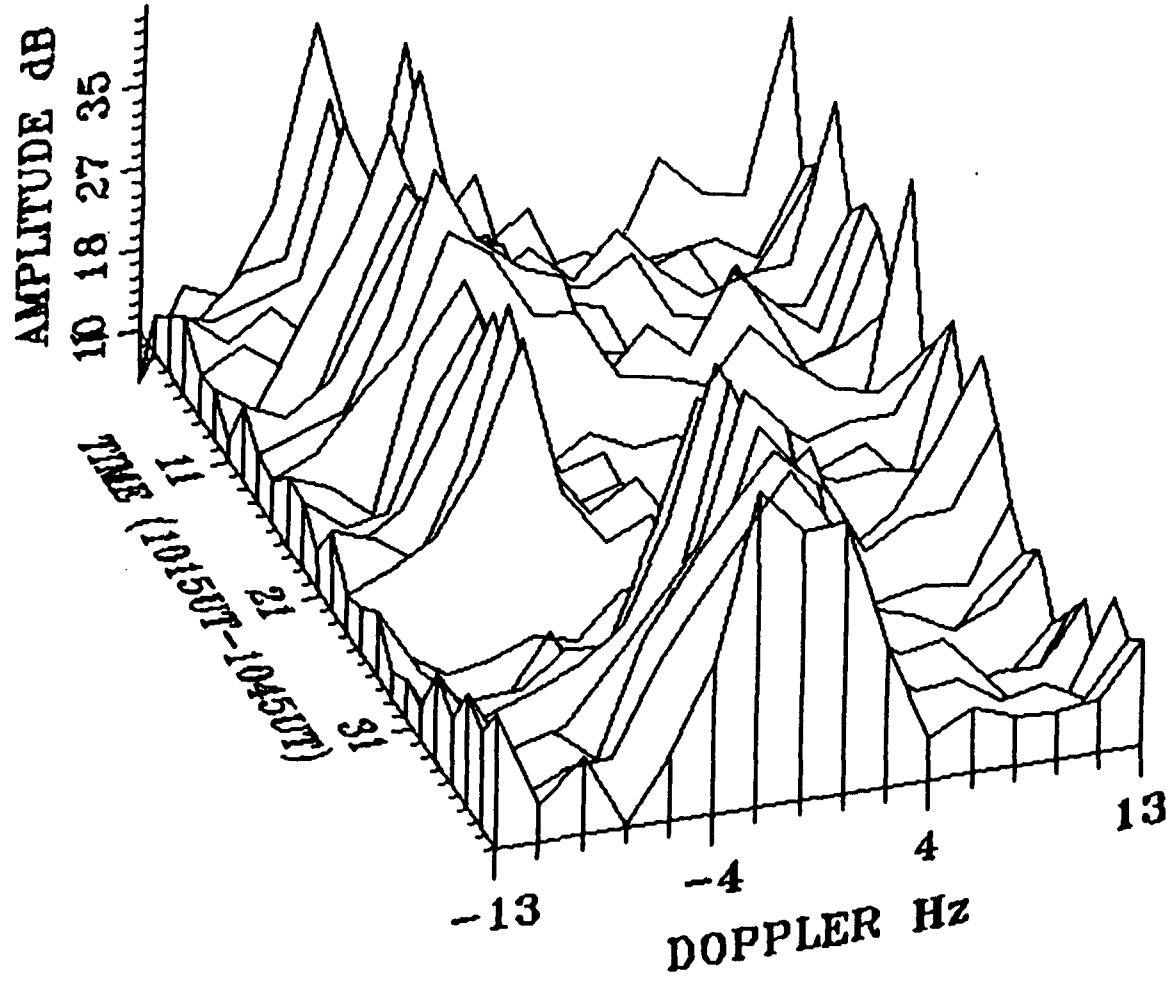

Figure 24. Doppler amplitude spectra, Digisonde Portable Sounder data recorded between 1015 to 1045 UT on 2 March 1993.

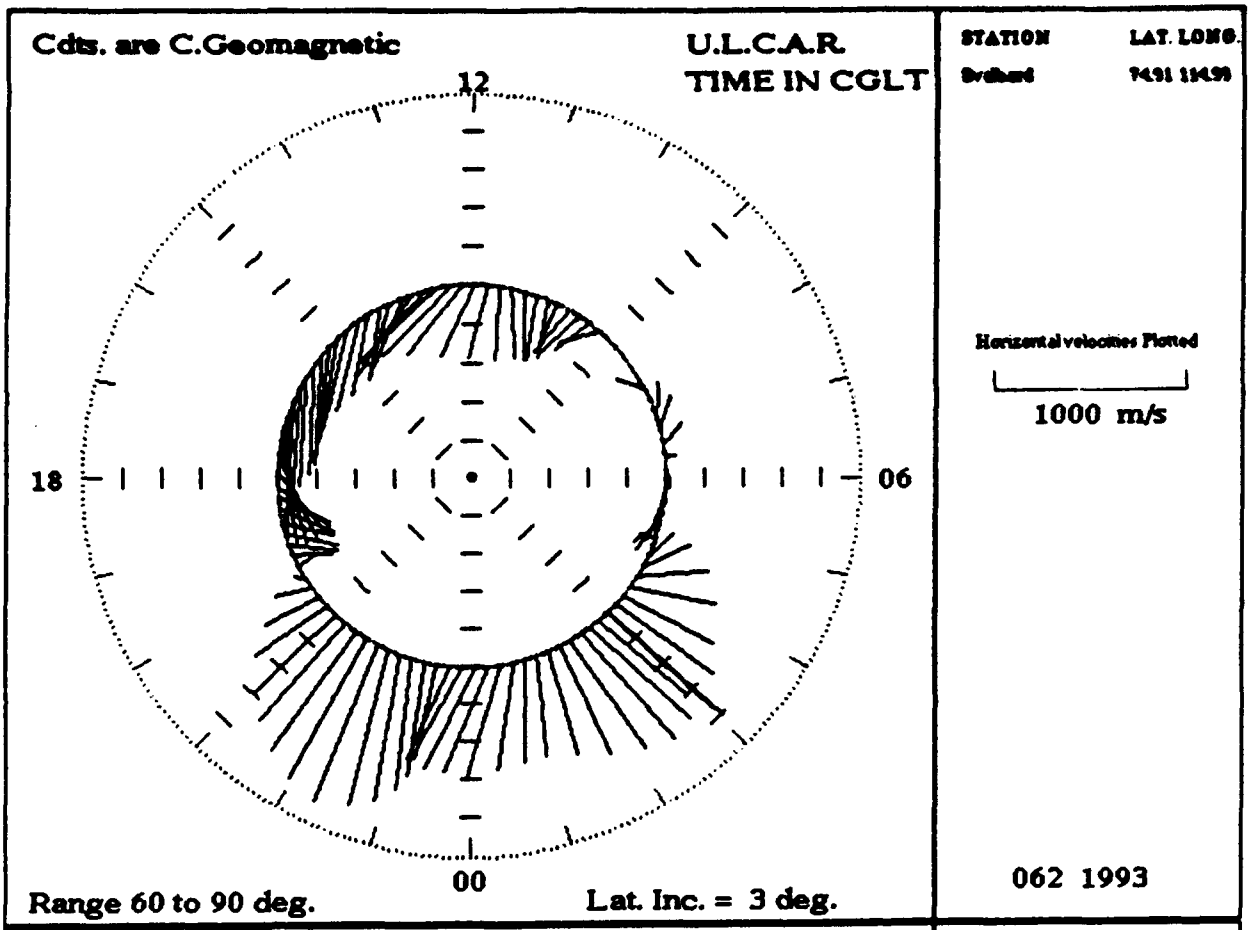

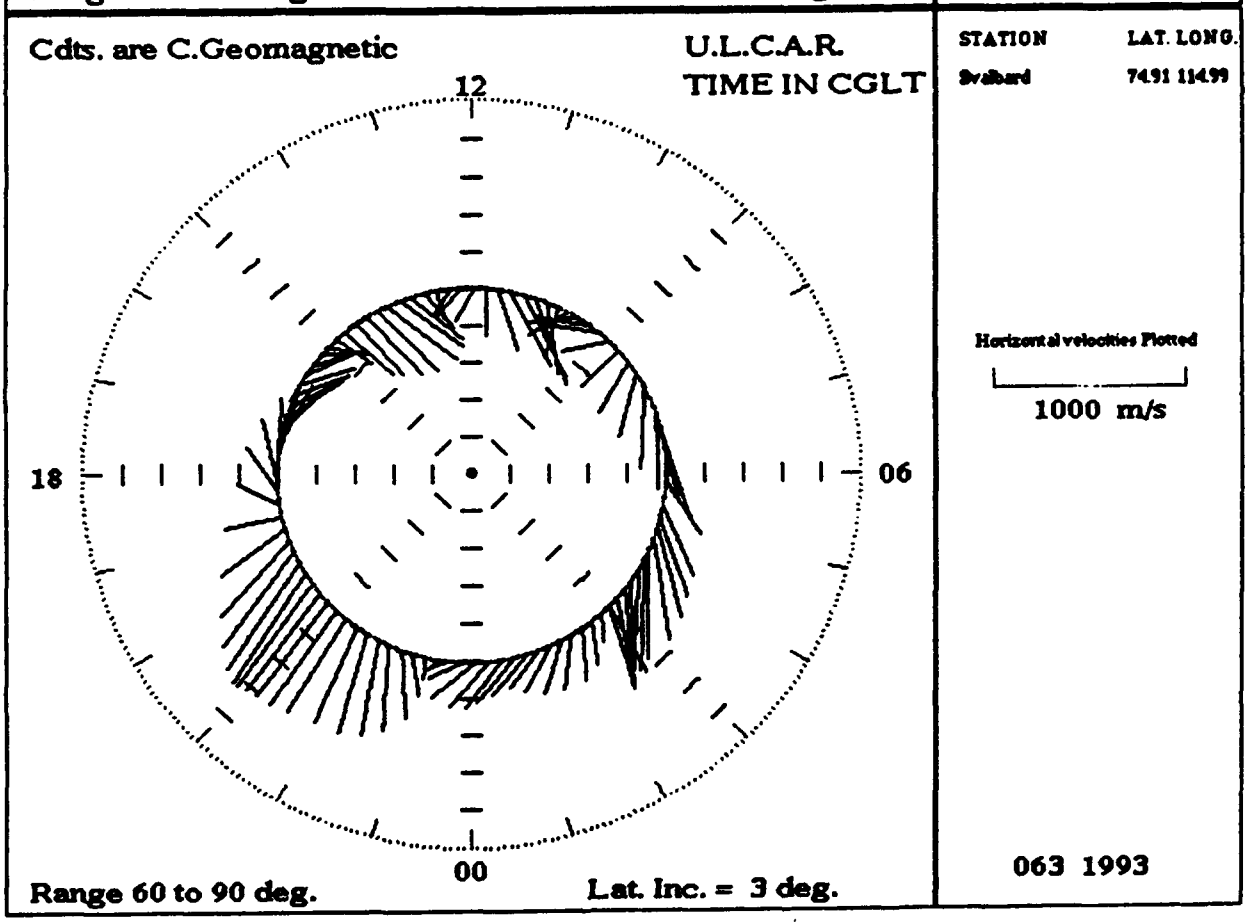

Figure 25. Polar plots of horizontal velocity components at Svalbard for days 62 and 63.

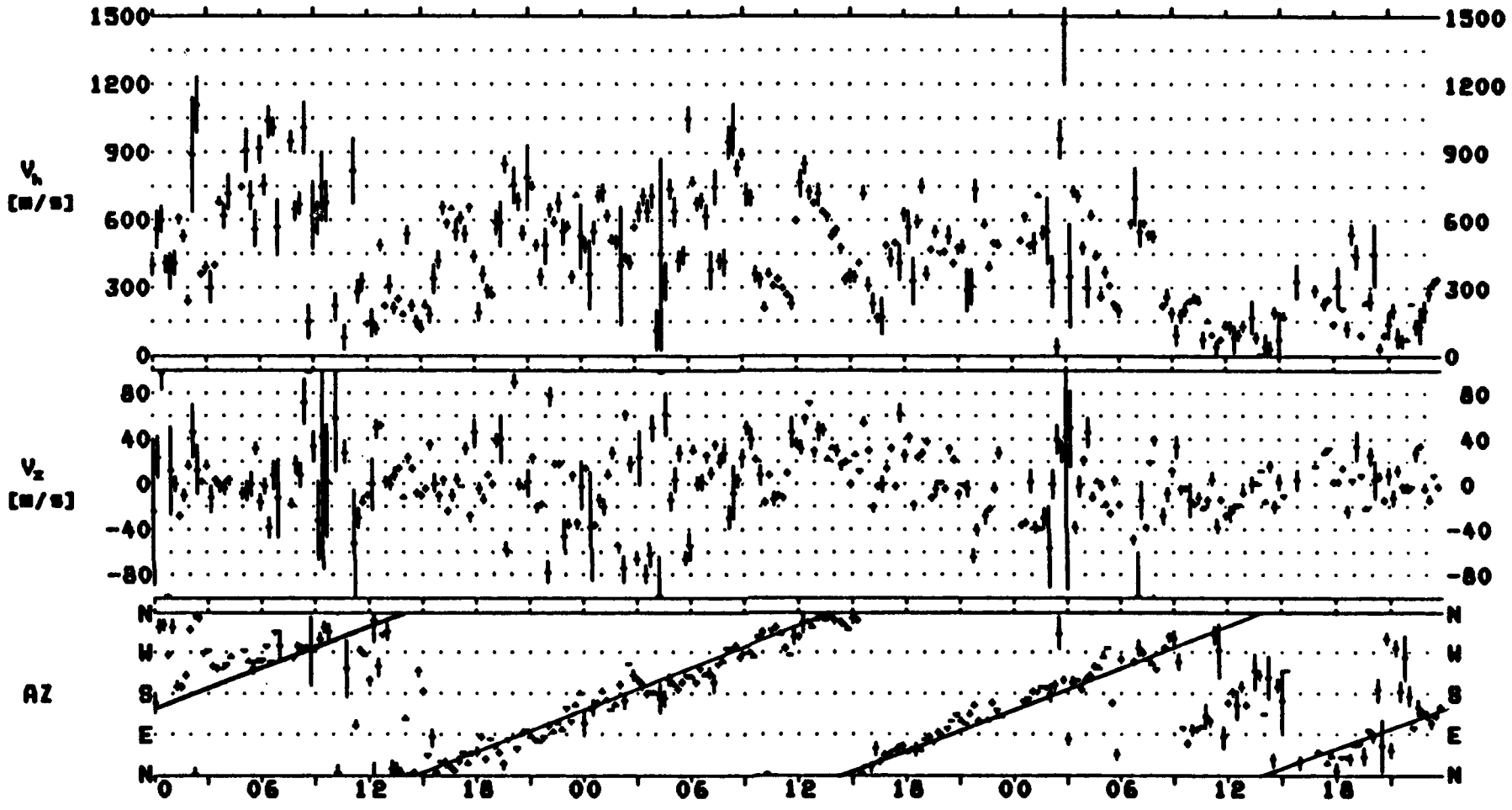

Figure 26. F region drift observed with the Digisonde 256 at Qaanaaq, Greenland, for days 61, 62 and 63, 1993.

Day 63 (Figure 21) shows a westward velocity from 0630 to 1330 UT and then the flow becomes antisunward until 1930 UT when the drift direction becomes irregular and v_h becomes small. Not observed is an eastward flow around 08 UT. A comparison with the Qaanaaq drift (Figure 26) gives a likely explanation. The Qaanaaq drift data indicate that Bz became positive from 08 to 17 UT on day 63. Shortly after 21 UT Bz seems to become positive again for a short while; surprisingly the Ny Alesund drift starts deviating from antisunward flow earlier than that.

For day 64 the Qaanaaq drift (Figure 27) shows a period of positive Bz from 11 to 15 UT, when it seems to turn negative again, since the drift at Qaanaaq becomes strictly antisunward. The Ny Alesund drift on day 64 (Figure 22) is very similar to the schematic sketch in Figure 18. At 08 UT the drift turns from eastward through northward to westward while Ny Alesund moves from the dawn cell through the cusp to the dusk cell. The westward velocity is maintained in the post-noon sector independent of the apparent change in Bz to positive from 11 to 15 UT. As on the previous days, the drift speed v_h increases from about 350m/s to 700m/s when Ny Alesund enters the polar cap and the flow becomes antisunward. The quick drop in v_h around 22 UT indicates a change in the interplanetary magnetic field. The Qaanaaq data (Figure 27) confirm this, the velocity drops and the flow is no longer antisunward.

To illustrate the variability of the convection pattern, the horizontal velocity v_h for Ny Alesund for days 62 and 63 has been replotted in polar form (Figure 25). For both days these polar plots clearly show antisunward convection in the night sector. Reversal boundaries are detected at 05 and 20 CGLT on day 62, but the situation is not so clear on day 63 when Bz during the daytime is switching between negative and positive according to the Qaanaaq drift (Figure 26). Similar to day 62, the drift becomes consistently antisunward around 20 CGLT (2230 UT). At this time, the Qaanaaq drift also becomes antisunward (Figure 26).

Drift data from the other high latitude Digisonde stations would allow to draw a more complete picture of the convection pattern. Future work will include the inputs from other stations in the mapping of the high latitude convection patterns.

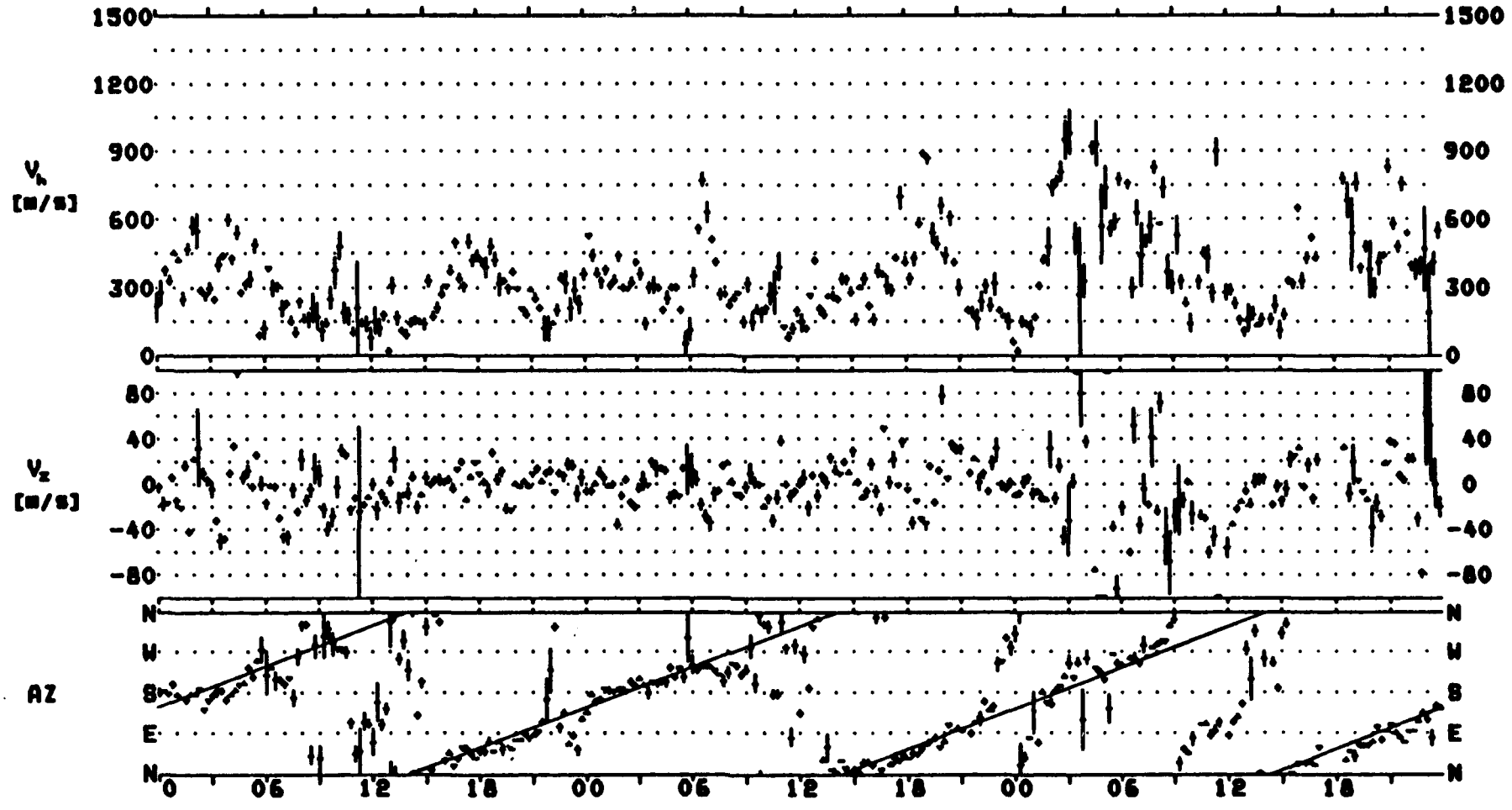

Figure 27. F region drift observed with the Digisonde 256 at Qaanaaq, Greenland, for days 64, 65 and 66, 1993.

5.0 REFERENCES

Buchau, J. B.W. Reinisch, D.N. Anderson, E.J. Weber and C.G. Dozois, "Poiar Cap Plasma Convection Measurements and Their Relevance to the Real Time Modelling of the High Latitude Ionosphere," Radio Science, 23, 4, pp. 521-536, July-August 1988.

Buchau, J. and B.W. Reinisch, "Electron Density Structures in the Polar F Region," Adv. Space Res., 11, 10, pp. (10)29-(10)37, 1991.

Buchau, J., Private Communication, 1992.

Cannon, P.S., B.W. Reinisch, J. Buchau and T.W. Bullett, "Response of the Polar Cap F Region Convection Direction to Changes in the Interplanetary Magnetic Field: Digisonde Measuements in Northern Greenland," J. Geophys. Res., 96, A2, pp. 1239-1250, 1991.

Hairston, M.R. and R.A. Heelis, "Model of the High-Latitude Ionospheric Convection Pattern During Southward Interplanetary Magnetic Field Using DE-2 Data," J. Geophys. Res., 95, pp 2000-2343, 1990.

Heppner, J.P. and N.C. Maynard, "Empirical Models of High Latitude Electric Field Models," J. Geophys. Res., 92, pp 4467-4489, 1987.

Reinisch, B.W., J. Buchau and E.J. Weber, "Digital Ionosonde Observations of the Polar Cap F Region Convection," Physica Scripta, 36, pp. 372-377, 1987.

Reinisch, B.W., D.M. Haines, W.S. Kuklinski, "The New Portable Digisonde for Vertical and Oblique Sounding", AGARD Proceedings Number 502, pp. 11-1 to 11-11, 1992.

Sojka, J.J., C.E. Rasmussen and R.W. Schunk. "An Interplanetary Magnetic Field Dependent Model of the Ionospheric Convection Electric Field," J. Geophys. Res., 91, pp 11281-11290, 1986.